UNCOVERING LOCAL MAGNETOSPHERIC PROCESSES GOVERNING THE MORPHOLOGY AND PERIODICITY OF GANYMEDE'S AURORA USING THREE-DIMENSIONAL MULTIFLUID SIMULATIONS OF GANYMEDE'S MAGNETOSPHERE

A Master's Thesis
Presented to
The Academic Faculty

by

Alexia Payan

In Partial Fulfillment
of the Requirements for the Degree
Master's in the
School of Earth and Atmospheric Sciences

Georgia Institute of Technology
May, 2013

UNCOVERING LOCAL MAGNETOSPHERIC PROCESSES GOVERNING THE MORPHOLOGY AND PERIODICITY OF GANYMEDE'S AURORA USING THREE-DIMENSIONAL MULTIFLUID SIMULATIONS OF GANYMEDE'S MAGNETOSPHERE

Approved by:

Dr. Carol Paty, Advisor
School of Earth and Atmospheric Sciences
Georgia Institute of Technology

Dr. Josef Dufek
School of Earth and Atmospheric Sciences
Georgia Institute of Technology

Dr. Irina Sokolik
School of Earth and Atmospheric Sciences
Georgia Institute of Technology

Date Approved: April 3rd, 2013

ACKNOWLEDGEMENTS

I wish to thank my advisor Dr. Carol Paty for her time, her kindness, and her enthusiasm. I also wish to thank Dr. Josef Dufek and Dr. Irina Sokolik for their valuable help and time. Finally, I would like to thank my family and my love for believing in me and for supporting me in my decision to pursue my passion for Space.

TABLE OF CONTENTS

LIST OF TABLES

LIST OF FIGURES

LIST OF SYMBOLS AND ABBREVIATIONS

a_0	Bohr's radius
B_G	Ganymede surface magnetic field
$B_{J\text{-}G}$	Jovian magnetic field at the distance of Ganymede
B	Brightness
$C(T_e)$	Collisional excitation rate
e	Elementary charge
E	Transition threshold energy
E_{thres}	Excitation threshold
F_s	Fraction of plasma species s that has an energy above the excitation threshold
n_e	Electron number density
n_s	Number density of species *s*
$N(O_2)$	Atmospheric column density of oxygen in Ganymede's atmosphere
P_e	Electron thermal pressure
R_J	Jovian Radius
R_G	Ganymede Radius
T_e	Electron temperature
v_s	Velocity of species *s*
$\eta\mathbf{j}$	Collisional resistivity of a plasma
μ	Bulk temperature
$\sigma(T_e)$	Cross section of electron impact dissociation of O_2
B	Magnetic field

E	Electric field
j	Electric current density

SUMMARY

Although magnetohydrodynamic (MHD) techniques are now being applied to the problems of fusion power and of confinement of hot plasmas by electromagnetic forces, the major application of MHD still concerns geophysical and astrophysical problems, especially those pertaining to space plasma physics. MHD is most commonly used in the single-fluid limit where the differences between particle species in a plasma are neglected such that the plasma can be regarded as a single conducting fluid carrying magnetic and electric fields and currents. In this context, MHD is an approximation to the multifluid theory of plasmas, where different particle species are treated separately. It is shown that in order to better understand the dynamics of Ganymede's magnetosphere and ionosphere in response to forcing from the co-rotating Jovian magnetospheric plasma, it is necessary to account for the various ion species and various plasma sources that comprise the global plasma population and energy distribution at Ganymede. Previously, researchers have used simplified versions of the generalized MHD equations to simulate and study Ganymede's magnetosphere. However, such ideal or resistive MHD models fail to incorporate particle drift motions and to predict the pick-up of ionospheric ions by incident magnetized plasma flows. As such, they are missing information about the resulting asymmetric flows and field morphologies, effects which are captured in the multifluid approach. In this research, a three-dimensional multifluid model is used and complemented by a brightness model to study the local magnetospheric processes responsible for the brightness and the morphology of the aurora at Ganymede depending on its position with respect to the Jovian plasma sheet. It is shown that the three-

dimensional multifluid model coupled with the newly developed brightness model predicts auroral brightnesses and morphologies that agree well with the observations of Ganymede's aurora by the Hubble Space Telescope. Our results also suggest the presence of short- and long-period variabilities in the auroral brightness at Ganymede due to magnetic reconnection processes on the magnetopause and in the magnetotail, and support the hypothesis of a correlation between the variability of Ganymede's auroral footprint on Jupiter's ionosphere and the variability in brightness and morphology of the aurora at Ganymede.

CHAPTER 1

INTRODUCTION

1.1. Jupiter's Magnetosphere

Jupiter is the largest and most massive planet in our solar system. It is located at 5.2 AU from the Sun, has an equatorial radius of ~71,600 km, a rotational period of 0.41354 Earth day or 9 hours 55 minutes and 29 seconds, and an orbital period of about 12 Earth years. Jupiter has a very strong magnetic field: at Jupiter's surface, it is roughly 10 times stronger than that at Earth's surface with an equatorial strength on the order of 428,000 nT. This magnetic field creates the strongest and largest planetary magnetosphere in the Solar System. Jupiter's magnetosphere extends from about 85 R_J upstream to more than 7,000 R_J downstream, and would appear 5 times larger than the Moon if it were visible in the night sky, as pictorially represented in Figure 1.

Figure 1: Jupiter's Magnetosphere (Credit: NASA/*Lunar and Planetary Institute-USRA*)

Jupiter's magnetic field is tilted by ~10° compared to its rotation axis. This makes the magnetosphere wobble around the planet and causes the central plasma sheet to flap up and down with respect to the ecliptic plane. This is depicted in Figure 2.

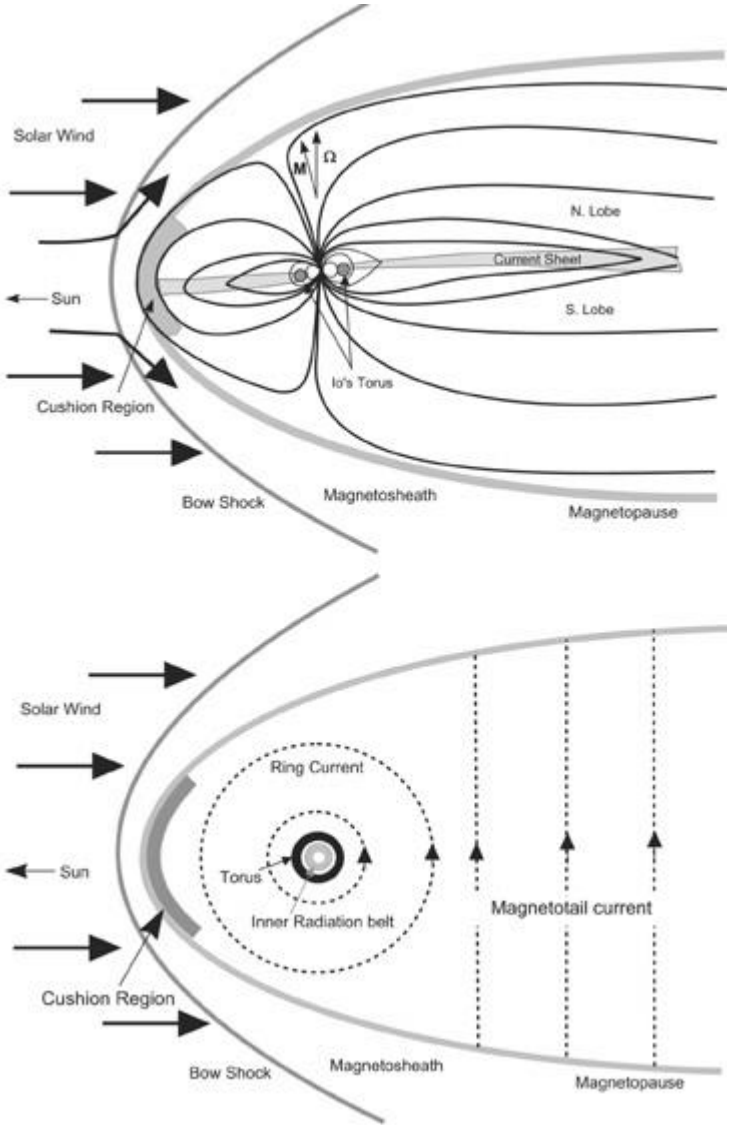

Figure 2: Jupiter's Magnetosphere (Credit: [*Bagenal et al.*, 2004]). The Top Figure is a Side View of the Magnetosphere and its Interaction with the Solar Wind. The Bottom Figure is a Top View on the Northern Hemisphere of the Magnetosphere and its Main Current Systems.

Jupiter is composed of dozens of moons, the four largest of which are the Galilean satellites Io, Europa, Ganymede and Callisto named after the Italian astronomer Galileo Galilei who observed them for the first time in 1610. These large Galilean moons are each unique. For instance, Ganymede is the largest moon in the Solar System and the only one to have its own intrinsic magnetic field. This creates a small magnetosphere inside of the large Jovian magnetosphere which features processes mimicking the interaction of the Solar Wind with the Earth magnetic field such as the precipitation of electrons in the ionosphere at the origin of majestic aurorae. Io is the most volcanically active body in the Solar System. As it travels along its slightly elliptical orbit, Io is heated by tidal forces resulting from the immense gravitational pull of Jupiter and the interaction with the harmonically orbiting icy moons of Europa, Ganymede and Callisto. As a result of tidal heating, Io's volcanic activity is the primary source of mass loading in the Jovian magnetosphere, releasing about one tonne of plasma per second which forms a torus around Jupiter at the orbit of Io which extends from approximately 5 R_J to 10 R_J from the planet's axis of rotation [*Schneider and Trauer*, 1995]. Europa is mostly covered by a layer of water ice that may overlay a sub-surface ocean of liquid water or slushy ice. It is thought to be composed of about twice as much water as that present on Earth and thus, may have a potential for harboring life. Finally, Callisto is a very ancient and heavily cratered world, providing a visible record of the early bombardment history of the Solar System. Although Callisto may look like a dead moon, the presence of a few small craters demonstrates a small degree of current surface activity [*Showman and Malhotra*, 1999].

Because of its extensive system of moons, Jupiter forms a kind of miniature solar system partially shielded from the Solar Wind. Indeed, while the planet is quite large, its rotation period is relatively small, ~10 hours. The plasma inside the magnetosphere starts corotating with the planet but the intense mass loading from Io causes the plasma to lag behind corotation between 15 and 20 R_J [*Krupp et al.*, 2004; *Khurana et al.*, 2004; *Russell*, 2001]. As a consequence, most of the magnetospheric dynamics is internally driven and the variable Solar Wind has little to no influence within 20 R_J where Ganymede, Europa, and Io are located [*Elkins-Tanton*, 2006]. Although the Galilean moons are almost completely protected from the variable effects of the Solar Wind, they are heavily bombarded with radiations and heavy magnetized plasma that sweeps past them at corotational speed. As mentioned earlier, Jupiter's magnetosphere wobbles relative to the orbital plane of the moons. Therefore, the thin and dense Jovian plasma sheet periodically flaps up and down over each moon every 10 hours, thus changing the local density significantly from very large values when the moon is inside the plasma sheet to very small values when the moon is outside of the plasma sheet. Similarly, the Jovian magnetic field strength in the vicinity of the moons varies from very weak inside the plasma sheet to very large outside of the plasma sheet. This variability modulates the Alfvén speed of the flow which governs the interaction of Ganymede's magnetosphere with the Jovian plasma, and the interaction of Io with the plasma in its torus.

1.2. Ganymede's Magnetosphere

Ganymede, third Galilean satellite of Jupiter and largest satellite in the Solar System, is the only moon-like body in the Solar System known to possess a

magnetosphere. Indeed, Galileo flybys of the Jovian system suggested that Ganymede generates its own internal magnetic field [*Kivelson et al.*, 1996, 1997, 1998], thus creating a mini-magnetosphere inside the larger Jovian magnetosphere. Inside the heliosphere, this currently constitutes the special and unique example of a magnetosphere embedded inside another magnetosphere, as shown in Figure 3.

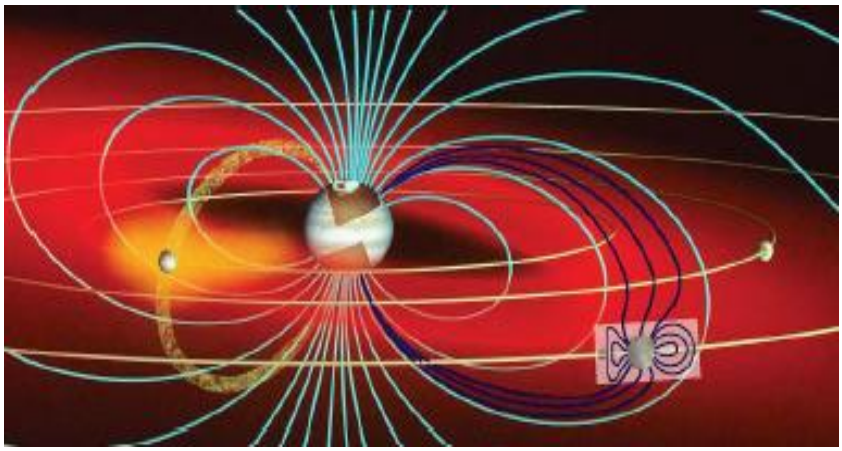

Figure 3: Ganymede's Magnetosphere Inside Jupiter's Magnetosphere (Left Moon is Io and Right Moon is Europa) (Credit: John Spencer, HST/NASA/ESA/J.C. Clarke, Outer Planet Flagship Mission/JPL)

The presence of a global magnetic field at Ganymede was inferred from the detection of radio emissions as the Galileo spacecraft approached Ganymede [*Gurnett et al.*, 1996] and was later confirmed by Galileo's magnetometer data during closer flybys of the moon [*Kivelson et al.*, 2002]. Extrapolations of the latter data also demonstrated the presence of both a strong intrinsic dipolar magnetic field and a time variable induced magnetic field, possibly due to the existence of a conductive subsurface ocean at Ganymede [*Kivelson et al.*, 2002].

The peculiar location of Ganymede's magnetosphere results in its interaction with the corotating sub-magnetosonic Jovian plasma. In this interaction, Jupiter's magnetic

field is driving the shape of Ganymede's magnetosphere and is responsible for the observation by the Hubble Space Telescope of oxygen airglow and aurora phenomena at Ganymede [*Hall et al.*, 1998; *Feldman et al.*, 2000]. Through the acceleration of electrons responsible for the generation of aurorae in both Ganymede's ionosphere and Jupiter's ionosphere [*Clarke et al.*, 2002], plasma dynamics is believed to play a significant role in the coupled interaction of Ganymede's mini-magnetosphere with the corotating magnetized plasma present in the larger Jovian magnetosphere, as depicted in Figure 4. The detection of plasma escaping from Ganymede's ionosphere [*Frank et al.*, 1997; *Eviatar et al.*, 2001] reinforces the importance of plasma dynamics in the description and understanding of the aforementioned interaction.

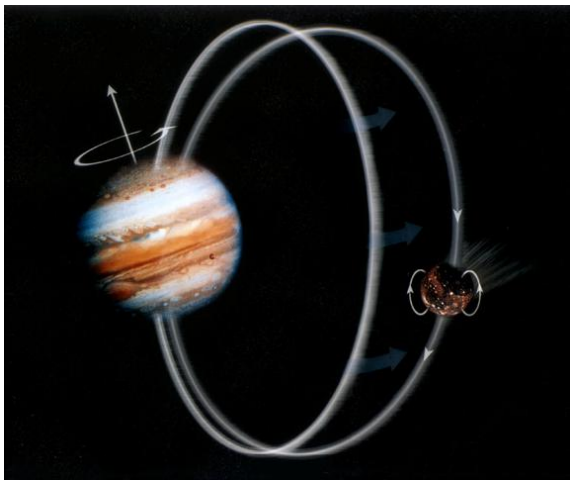

Figure 4: Interaction Between Jupiter and Ganymede Through Plasma Waves (Credit: NASA/JPL)

1.3. Magnetohydrodynamics

MHD is a field of study initiated by the Swedish electrical engineer and plasma physicist Hannes Alvfén, for which he received the Nobel Prize in Physics in

1970. Most generally, MHD is the fluid theory of electrically conducting media subject to the presence of external and internal magnetic fields. In other words, it is the study of the dynamics of a fluid moving in an electromagnetic field, where currents established in the fluid by induction modify the field itself, so that the field and dynamic equations are coupled.

The simplest example of an electrically conducting fluid is a liquid metal, such as mercury or liquid sodium, but effects of interactions between moving conducting fluids with electric and magnetic fields can also be observed in gases and two-phase mixtures. Nevertheless, the study of MHD was primarily motivated by its widespread application to the description of magnetized bodies within the Solar System and astrophysical plasmas within and beyond the Solar System. Although MHD has been recently called upon to tackle the problem of fusion power involving the creation and containment (confinement) of hot plasmas by electromagnetic forces [*Tillack and Morley*, 1998; *Thorne*, 2008; *Calvert*, 2011], the major use of MHD still concerns geophysical and astrophysical problems. Geophysical problems include planetary magnetism, believed to be the result of a dynamo action produced by complex fluid motions and currents within the planet's liquid core. For instance, Glatzmaier and Roberts [*Glatzmaier and Roberts*, 1995] have used MHD to study the geomagnetic dynamo at Earth by developing a supercomputer model of the Earth's interior. The simulations show the expected changes in the Earth's magnetic field over thousands of years in virtual time, and correctly predict the flips in the Earth's magnetic field that occur every few thousands of years. This is depicted in Figure 5.

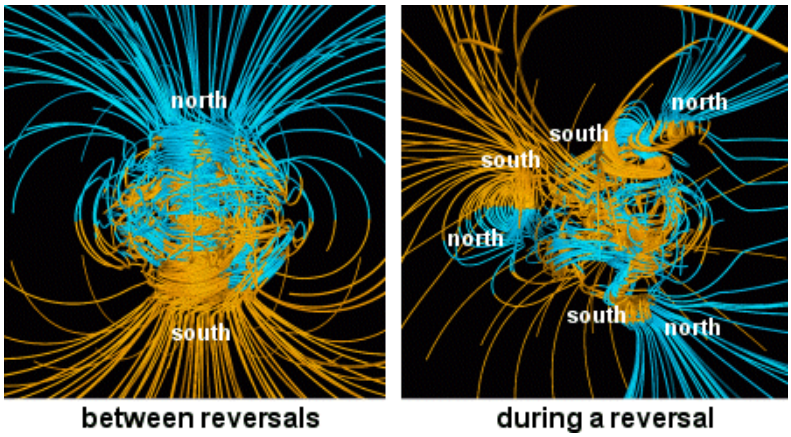

Figure 5: Earth's Magnetic Field Reversals (Credit: [*Glatzmaier and Roberts*, 1995] NASA/JPL)

Astrophysical problems include solar structure (especially in the outer layers of the Sun), interaction of the solar wind with magnetized planets and moons, and interstellar magnetic fields. For example, sunspots are caused by the Sun's magnetic field looping over its photosphere, as Joseph Larmor theorized in 1919 [*Larmor*, 1919]. The Sun may be regarded as a hot plasma bubble whose equator rotates faster than its poles. This differential rotation is responsible for the wrapping of the closed magnetic field lines around the surface of Sun, and for the creation of magnetic loops in regions of large magnetic stresses. This is displayed in Figure 6.

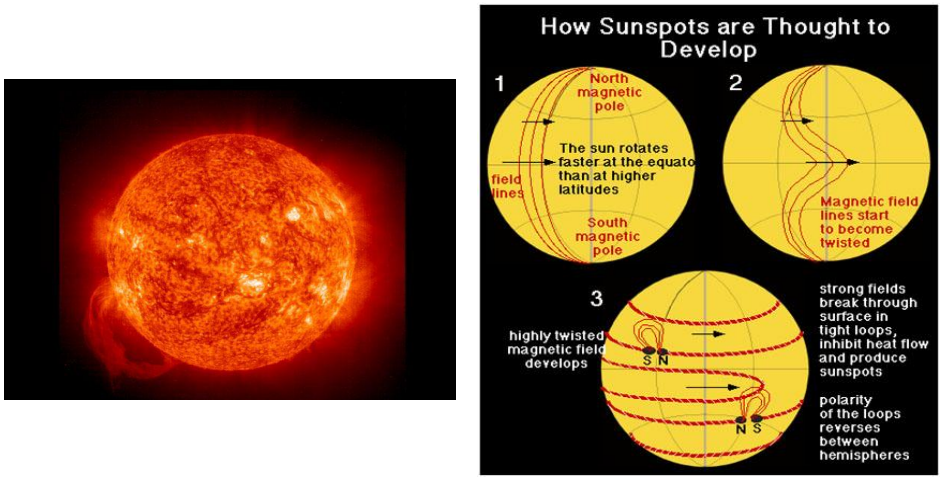

Figure 6: Magnetic Loop and Sunspots (Credit: NASA/SOHO, National Geographic)

This differential solar rotation may also be the long term effect of magnetic drag at the poles of the Sun, a MHD phenomenon due to the open magnetic field lines spiraling as they extend outward from the Sun's poles [*Wilcox et al.*, 1980; *Smith*, 1999]. This is displayed in Figure 7.

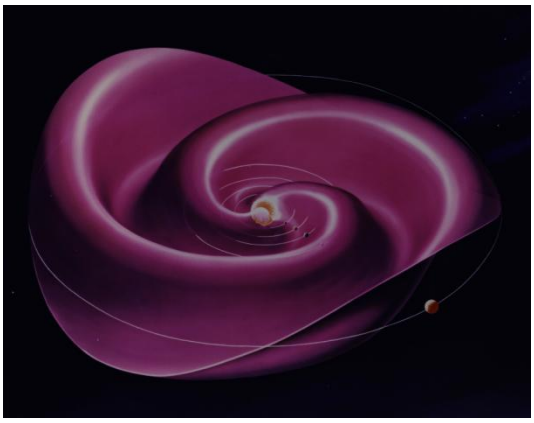

Figure 7: Propagation of the Solar Wind Along the Parker Spiral (Credit: NASA/Werner Heil)

Another example of MHD treatment of astrophysical problems would be plasma physics which turns out to be of uttermost importance in our study of Ganymede's magnetospheric population and energy distribution.

A plasma may be regarded as a hot, quasi-neutral ionized gas containing free electrons and multiple ion species, including negative ions as well as neutral particles. A plasma is electrically conductive. Therefore, it couples to electric and magnetic fields to create a complex structure which supports the propagation of a wide variety of plasma waves. Since the mean free paths for collisions between charged particles in a plasma are macroscopically long, it is by no means obvious that plasmas can be treated as fluids [*Baumjohann and Treumann*, 2006]. Nevertheless, the particle velocity distributions can

be isotropized locally by electromagnetic (when there is an oscillating magnetic field) or electrostatic waves propagating through the plasma. In that sense, the plasma can be sensibly described by a macroscopic mean density, velocity and pressure [*Thorne*, 2008]. Then, it can be shown that these mean quantities obey the same conservation laws of mass, momentum and energy as regular fluids encountered in the domain of fluid and gas dynamics.

In order to better understand the phenomena at play in Ganymede's magnetosphere and ionosphere in response to forcing from the corotating Jovian magnetospheric plasma, it is necessary to account for the various sources of plasma composing the global plasma population and the resulting energy distribution at Ganymede [*Paty et al.*, 2008]. Previously, researchers have used simplified versions of the generalized MHD equations to simulate and study Ganymede's magnetosphere [*Stone and Armstrong*, 2001; *Kopp and Ip*, 2002; *Ip and Kopp*, 2002; *Jia et al.*, 2008, 2009]. For instance, resistive MHD studies demonstrated the effects of the orientation of the incident Jovian magnetic field on the morphology of Ganymede's magnetosphere, but did not model observed plasma dynamic perturbations to Ganymede's magnetic field due to various ion sources [*Kopp and Ip*, 2002; *Ip and Kopp*, 2002; *Jia et al.*, 2008, 2009]. On the contrary, Paty and Winglee [*Paty and Winglee*, 2004, 2006; *Paty et al.*, 2008] argued that a multifluid approach is better suited to resolve the heating and interaction of different ion species and sources within Ganymede's magnetosphere. More precisely, the multifluid approach incorporates particle drift motions and predicts the pick-up of ionospheric ions by incident magnetized plasma flows. The resulting asymmetric flows

and field morphologies are then fully captured in the multifluid equations, effects which are not predicted by resistive MHD models.

1.4. Validity of Magnetohydrodynamics at Ganymede

Compared with Earth, Ganymede is small (R_G =2,631 km) and has a weak surface magnetic field (B_G = 750 nT), about 50 times smaller than Earth's surface magnetic field. This surface magnetic field is nevertheless larger than the Jovian magnetic field at the distance of Ganymede (B_{JG} = 100 nT). Due to the small orbital speed of Ganymede (about 11 km/s), the corotating Jovian plasma impinges on Ganymede from its upstream side at a speed of about 180 km/s. In this case, the ambient plasma is a low-beta plasma such that the magnetic pressure dominates both the dynamics pressure and the thermal pressure. This is however not the case when Ganymede is near the center of the Jovian plasma sheet where the plasma beta exceeds one (usually about 1.6, cf G8 Galileo flyby of Ganymede [*Jia et al.*, 2008]). Indeed, the Jovian magnetotail neutral sheet is characterized by strong currents and small magnetic fields which results in a high-beta plasma. Figure 8 shows the value of the Jovian plasma beta depending on the relative position of Ganymede with respect to Jupiter's plasma sheet (Ganymede not to scale).

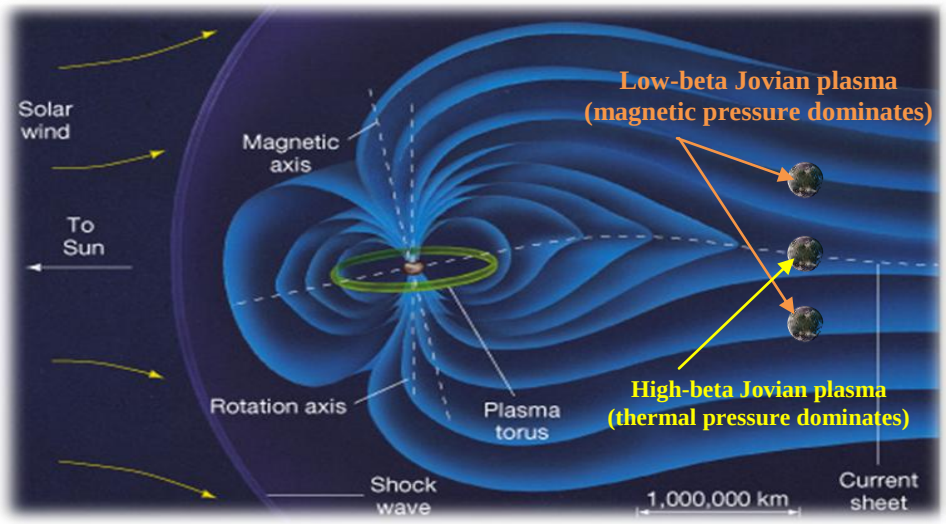

Figure 8: Jovian Plasma Beta at Ganymede (Modified From [*Pearson Prentice Hall Inc.*, 2005])

The Jovian magnetospheric plasma therefore drives Ganymede's magnetospheric and ionospheric processes responsible for the detection of an oxygen airglow and an aurora [*Hall et al.*, 1998], as well as of a hydrogen exosphere extending out to two Ganymede radii [*Feldman et al.*, 2000]. The aurora at Ganymede is most probably produced by dissociative impact excitation of atmospheric O_2 molecules from precipitating electrons. The observed brightness of Ganymede's auroral footprint at Jupiter (order of tens of kilorayleighs) [*Clarke et al.*, 2002] confirms the strong interaction between Ganymede's magnetosphere and the corotating Jovian magnetospheric plasma. In particular, Frank et al. [*Frank et al.*, 1997] reported that, as the Galileo spacecraft traversed Ganymede's Polar Regions, it detected strong ionospheric outflows of H^+ and O^+ ions. These outflows of ions from Ganymede's ionosphere actually balance the inflow of Jovian magnetospheric particles due to the reconnection of Ganymede's magnetic field with Jupiter's magnetic field and responsible for the generation of the aurora at Ganymede. These outflowing ions are then picked up

by the incident Jovian magnetized plasma and create asymmetries in the morphology of the flow and of the magnetic field.

In order to fully understand the plasma environment of Ganymede and its magnetic signatures, it is necessary to account for Ganymede's ionospheric composition and density. This implies being able to discriminate the different sources of ions in the near-Ganymede plasma environment.

Several researchers have used resistive MHD to study the effects of variations in the incident Jovian magnetic field configuration on Ganymede's magnetospheric and ionospheric processes [*Kopp and Ip*, 2002; *Ip and Kopp*, 2002; *Jia et al.*, 2008, 2009]. In this approximation, all length-scales of variations are required to be longer than the ion gyroradius such that the associated ion drift motions, resulting from diffusion of the magnetic field through the ion plasma fluid, are negligible. However, this is not the case at Ganymede, where the ion gyroradius of the major component ion O^+ can vary from 400 km in the incident Jovian plasma flow to many thousands of kilometers near reconnection regions where the magnetic field becomes very weak [*Neubauer*, 1998]. In this case, the ion gyroradius is larger than relevant length-scales, mainly the height of the ionosphere (125 km), Ganymede's radius (2,631 km), and the altitude of the magnetopause above Ganymede's surface (2236-4788 km) [*Paty and Winglee*, 2006]. Hence, the very fact that the near-space environment of Ganymede is populated by several ion species with large gyroradii traveling in weak magnetic fields invalidates a general assumption of the ideal MHD and of the resistive MHD, despite it already being a relaxation of the ideal MHD for collisional plasmas. In this case, a multifluid treatment is required. In such an approach, different ion species are regarded as separate fluids such

that the heating of these different ion species and sources and their interactions with Ganymede's magnetosphere and ionosphere may be resolved. As another consequence, the large ion gyroradii resulting from the weak magnetic fields encountered at Ganymede are perfectly incorporated into the multifluid theory [*Paty and Winglee*, 2004, 2006]. The validity of the MHD approximation in Ganymede's magnetosphere is indicated in Figure 9.

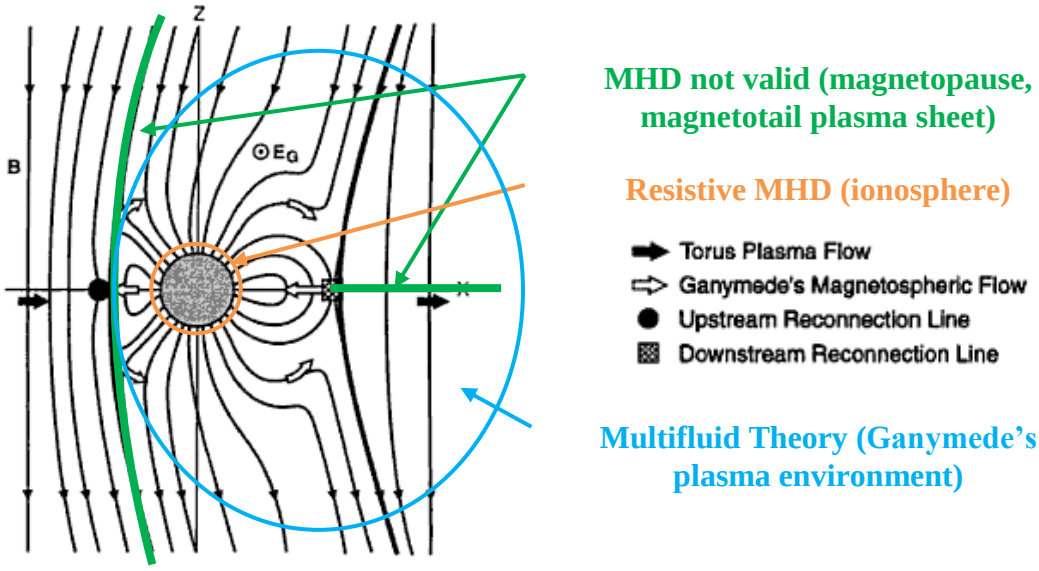

Figure 9: Validity of MHD at Ganymede (Modified From [*Ohtani et al.*, 1999])

To conclude, Paty and Winglee [*Paty and Winglee*, 2004, *Paty*, 2006; *Paty et al.*, 2008] showed that a multifluid model of Ganymede's near-space environment agrees well with magnetic field data from the Galileo spacecraft magnetometer and with ion energy distributions provided by the Galileo Plasma Wave Experiment. The model further predicts auroral features comparable to ultraviolet images of Ganymede's aurora obtained by the Hubble Space Telescope. More precisely, Paty and Winglee assessed the

validity of their multifluid model against observed and extrapolated quantities such as the strength of the magnetic field, the sputtering rates of H^+ and O^+ ions, the location of the aurora, and the structure of Ganymede's magnetosphere [*Paty and Winglee*, 2004]. They further noticed that a multifluid approach allows tracking the motion and energization of various ion species in the incident Jovian magnetospheric plasma, so that the interaction of these incident heavy ions with Ganymede's magnetosphere and ionosphere and their role in sputtering ions from Ganymede's surface may be monitored [*Ip et al.*, 1997; *Paranicas et al.*, 1999]. In a similar context, Paty [*Paty*, 2006] found that, in order to consistently describe the magnetic field configuration at Ganymede and the dynamics behind the size and shape of its magnetosphere, it was necessary to fully account for the physics associated with heavy ion gyromotions. As a conclusion, in order to be able to investigate the ion population and energy distribution within Ganymede's magnetosphere, a multifluid treatment of Ganymede's near-space plasma environment is required. Such a multifluid approach allows the concurrent examination and the accurate prediction of the interaction between Ganymede's ionospheric outflows of H^+ and heavy O^+ ions with the incident heavy ions corotating with the Jovian magnetospheric plasma.

1.5. Motivation

The electrodynamic interaction of Ganymede's mini-magnetosphere with Jupiter's corotating magnetospheric plasma has been shown to give rise to strong current systems closing through the moon and its ionosphere as well as through its magnetopause and magnetotail current sheet. This interaction is strongly evidenced by the presence of aurorae at Ganymede and Ganymede's bright auroral footprint on Jupiter's ionosphere.

The brightness of Ganymede's auroral footprint at Jupiter along with its latitudinal position have been shown to depend on the position of Ganymede relative to the Jovian plasma sheet and on the upstream magnetic field conditions in the Jovian plasma. Previous studies based on ultraviolet images obtained with the Hubble Space Telescope (HST) have demonstrated that the size of the auroral footprint mapped to a region corresponding to Ganymede's magnetosphere and not just to the moon. In addition, it was recently shown that Ganymede's auroral footprint brightness is characterized by three timescales of variations: a long 5-hour periodic variation, a non-systematic 10-40-minute variation, and a short 100-second quasi-periodic variation [*Grodent et al.*, 2009]. As for Ganymede's aurora, observations with the HST revealed longitudinally non-uniform oxygen emissions, with the brightest emissions confined to the geomagnetic latitudes defining the boundaries of the polar caps [*Feldman et al.*, 2000].

1.6. Scope of Thesis

This Master's thesis looks to further our understanding of the complex interactions between Ganymede's and Jupiter's magnetospheres initiated by the three-dimensional multifluid simulation model developed by Paty and Winglee [*Paty and Winglee*, 2004, *Paty*, 2006; *Paty et al.*, 2008]. By coupling the three-dimensional multifluid simulation model to a specifically designed brightness model, it is possible to unveil local magnetospheric processes governing the morphology and periodicity of Ganymede's aurora depending on its position with respect to the Jovian plasma sheet.

Chapter 2 will describe the three-dimensional multifluid simulation model used in this thesis and will refer to the original papers for more details about the specifics of the model.

Chapter 3 will describe the brightness model developed to calculate the brightness of the aurora at Ganymede using electron data provided by the multifluid simulation model and atmospheric conditions at Ganymede adapted from values published in the literature. First, some generalities about Ganymede, its aurora, and the main observations of Ganymede's auroral emissions from the Hubble Space Telescope will be presented. Second, the brightness model will be described in details. The main parameters involved in the brightness calculation will be investigated before the model may be applied to Ganymede's aurora.

Chapter 4 will investigate the periodicity of the brightness and the morphology of the aurora at Ganymede, as well as the main sources of electrons generating the auroral emissions. The short- and long-period variability of the brightness and morphology of the aurora will then be explored and compared to ultraviolet observations from the Hubble Space Telescope. The component of the electric field parallel to the Ganymedian magnetic field will be examined in order to study the relationship between acceleration structures and precipitation of electrons in Ganymede's ionosphere. Finally, the morphology of the field-aligned currents will be investigated. This provides a way to visualize the separatrix region between open and closed magnetic field lines and allows the identification of the source regions of electrons generating the aurora at Ganymede.

CHAPTER 2

THREE-DIMENSIONAL MULTIFLUID SIMULATION MODEL

The present work builds on previous efforts by Paty and Winglee who developed a three-dimensional multifluid simulation model to better understand the complex interaction of Ganymede's magnetosphere with the Jovian plasma. For detailed information about the parameterization of the model, its boundary conditions, its assumptions, and its use, refer to [*Paty and Winglee*, 2004; *Paty*, 2006; *Paty and Winglee*, 2006; *Paty et al.*, 2008].

2.1. Description of the Multifluid Model and Relevant Literature

In order to study the variability in the morphology and the brightness of the aurora at Ganymede, it is necessary to regard different ion species as separate fluids such that the heating of these different ion species and sources and their interactions with Ganymede's magnetosphere and ionosphere may be resolved. This is done through the use of a three-dimensional multifluid model of Ganymede's near-space environment. In this model, different ion species are represented as collisionless fluids interacting via electric and magnetic fields. The multifluid approach treats the ionospheric species (O^+ and H^+) and the Jovian magnetospheric plasma (H^+, S^+, S^{2+}, O^+ and O^{2+} treated as a single fluid of heavy ions) as different entities, and allows tracking the motion and energization of these ion species in the incident Jovian magnetospheric plasma. This way, the interaction of these incident heavy ions with Ganymede's magnetosphere and ionosphere may be monitored. The three-dimensional modeling technique shows that the gyromotion of heavy ions governs the shape and the dynamics of Ganymede's magnetosphere, as well as the morphology of Ganymede's aurora. The multifluid model also allows tracking the simulated ion energies, temperatures, and densities for each ion

sources in Ganymede's magnetosphere and in the Jovian plasma. In this context, it is worth noting that the fluid simulations directly model average plasma properties, such as average energy, temperature, and density. This information may be used to derive the corresponding average energies, temperatures, and densities of electrons originating from the Jovian plasma and from Ganymede's magnetotail, and precipitating into Ganymede's ionosphere to generate the aurora. These average energies, temperatures, and densities may then be used to develop a brightness model enabling the study of the morphology and the brightness of the aurora at Ganymede, both on the Jovian flow facing side and on the Ganymede's magnetotail side, as Ganymede orbits around Jupiter. This provides information on the variability of Ganymede's aurora for several local Jovian magnetic field conditions corresponding to various positions of Ganymede with respect to the Jovian plasma sheet. This further provides information on the morphology of the aurora at Ganymede for different properties and precipitation schemes of both Jovian and magnetospheric electrons. In this context, it is worth mentioning that the multifluid model has been validated against Galileo magnetometer data for all three positions of Ganymede with respect to the Jovian plasma sheet considered in this research (above, at the center, and below, cf. Table 1 section 3.2.1.). Finally, the three-dimensional multifluid treatment of Ganymede's magnetosphere does not require the introduction of an anomalous resistivity as does resistive MHD [*Jia et al.*, 2008; *Jia et al.*, 2009]. The only resistivity encountered in the multifluid model concerns the ionospheric region which naturally features conductive current systems.

2.2. Goal of the Study

The present study looks to further our understanding of the brightness and the morphology of the aurora at Ganymede for various positions of Ganymede with respect to the Jovian plasma sheet. The goal of the study is to examine the periodicities in the brightness and the morphology of the aurora at Ganymede and the responsible local

processes occurring at the moon so as to relate the above to the observed short- and long-period variability of Ganymede's auroral footprint at Jupiter [*Grodent et al.,* 2009]. The objective of this work is thus to identify the source regions of electrons generating the aurora at Ganymede through dynamic reconnection processes occurring locally to the moon, and to relate those regions to the variability in the brightness and the structure of the auroral emissions at Ganymede.

In order to do so, a brightness model is created and coupled to the three-dimensional multifluid model developed by Paty and Winglee [*Paty and Winglee*, 2004]. The three-dimensional multifluid model tracks the different plasma populations responsible for the aurora and characterizes the interaction between Ganymede's magnetosphere and the incident Jovian plasma, thus determining the morphology of Ganymede's aurora. The brightness model further captures the relationship between the temperatures and densities of precipitating electrons and the atmospheric column density of oxygen molecules present in Ganymede's ionosphere to determine the strength of Ganymede's aurora. The dependency between precipitating electron temperatures and brightness of the aurora is evident through a coefficient of dissociative impact excitation [*Kanik et al.*, 2003] which represents the ability of precipitating electrons to produce excited oxygen atoms that will liberate photons as they release their additional energy, thus producing the aurora.

The information provided by the coupled model may then be used to understand the dynamics of Ganymede's magnetosphere in response to varying upstream Jovian magnetospheric conditions, to provide insight into the variability in the brightness and morphology of Ganymede's aurora, and to examine any correlation with the variability of Ganymede's auroral footprint on Jupiter's ionosphere.

CHAPTER 3

BRIGHTNESS MODEL

3.1. Introduction

3.1.1. Ganymede's Aurora

The peculiar location of Ganymede's magnetosphere inside the larger Jovian magnetosphere results in its interaction with the corotating sub-magnetosonic Jovian plasma. In this interaction, Jupiter's magnetic field is driving the shape of Ganymede's magnetosphere and is responsible for the observation by the Hubble Space Telescope (HST) of oxygen airglow and aurora phenomena at Ganymede [*Hall et al.*, 1998; *Feldman et al.*, 2000; *Retherford*, 2009]. More precisely, the HST/Goddard High Resolution Spectrograph (GHRS) detected emissions at the atomic oxygen multiplets O I] λ1304 and O I] λ1356 whose intensity ratio is the signature of electron dissociative excitation of molecular oxygen. It was also observed that the Ganymede O I] λ1356 emission line exhibited a double-peaked structure with the strongest emissions coinciding with Ganymede's Polar Regions [*Hall et al.*, 1998].

Figure 10 depicts ultraviolet images of O I] λ1356 emission for four contiguous orbits of the HST on October 30th 1998 (indicated by ABCD) on the Jovian flow facing side of the moon. At that time, Ganymede was about 4.25 AU from Earth, its sub-Earth longitude was between 290° and 300°, and the phase angle was 8.6°. In Figure 10, brightness contours are in Rayleighs (R) and the compass indicates the Jovian North (JN), the direction to Jupiter (J) and the anti-direction of the Jovian magnetic field (B). Figure 10 shows that Ganymede's auroral emissions are longitudinally non-uniform and that the resulting brightness varies from 50 R to 300 R depending on the latitude. It further depicts that the brightest emissions are confined to geomagnetic latitudes defining the

boundaries of the polar caps, above 40° latitude in both the Northern and the Southern hemispheres [*Feldman et al.*, 2000]. These regions correspond to the separatrix between open and closed magnetic field lines. These observed auroral emissions may be explained by the reconnection of the Jovian magnetic field lines with the open magnetic field lines of Ganymede on its magnetopause, at latitudes poleward of the separatrix region. Such local reconnection processes are responsible for the creation of the aurora on the flow facing side of Ganymede where the Jovian plasma sources can penetrate into Ganymede's ionosphere through the cusps above the separatrix. Over the four orbits of the HST, the Jovian magnetic field strength and direction relative to the Ganymede's magnetic field varied significantly, thus changing the location of the separatrix regions and of the Polar Regions on the surface of Ganymede over a Jovian rotation. This explains why auroral emissions at Ganymede exhibit considerable changes in latitudinal locations and brightnesses between the Northern and the Southern hemispheres as the moon rotates around Jupiter, and as its position with respect to the center of the Jovian plasma sheet varies.

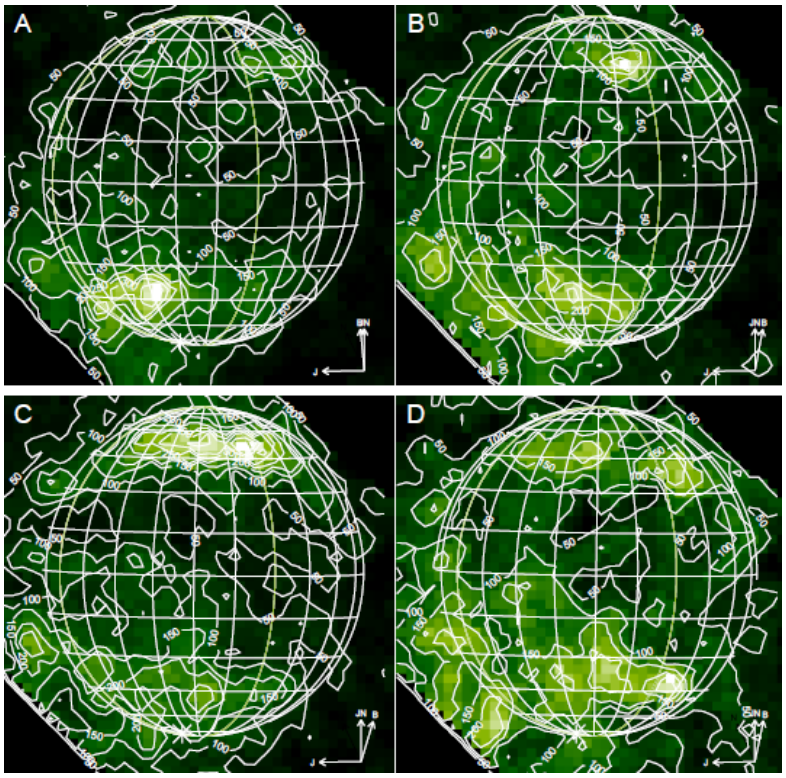

Figure 10: Ganymede's Aurora on the Jovian Flow Facing Side for Four Jovian Magnetic Field Configurations (Extracted From [*Feldman et al.*, 2000])

The newly reconnected open magnetic field lines then convect to Ganymede's magnetotail where they reconnect one more time as they are pushed back against each other by the magnetic pressure exerted by the Jovian plasma flowing around Ganymede. These secondary local reconnection processes are responsible for the generation of acceleration regions through which Ganymede's magnetospheric plasma sources can gain energy, travel along the newly reconnected closed magnetic field lines, and precipitate into Ganymede's ionosphere at latitudes below the separatrix [*Paty and Winglee*, 2004]. Figure 11 shows four sets of ultraviolet observations of the atomic oxygen emission line O I] λ1356 at Ganymede obtained from the HST/Space Telescope Imaging Spectrograph (STIS) in 1998, 2000, and 2003, and from the HST/Advanced Camera for Surveys Solar Blind Channel (ACS/SBC) in 2007 [*Retherford*, 2009; *McGrath et al.*, 2013]. The 1998 data are similar to those presented Figure 10. Figure 11 provides three different views of

Ganymede's aurora: the upper left figure represents a magnetotail side view, the lower left figure corresponds to the Jovian flow facing side view, and the two figures to the right provide a Jovian facing side view of Ganymede's aurora. In Figure 11, brightness contours are in Rayleighs (R) and the compass indicates the Jovian rotation axis (z), the direction to Jupiter (y) and the direction of the Jovian plasma flow impinging on Ganymede (x). Figure 11 shows that the brightness emissions are longitudinally and latitudinally non-uniform and range from 100 R to 400 R. In addition, it can be noticed that the auroral emissions are brightest at higher latitudes on the Jovian flow facing side compared to the magnetotail side where the aurora is mainly located below the separatrix between 10° and 20° latitudes. Nevertheless, the latitudes of emissions are uncertain by 10-15°. This further suggests that the main source of electrons generating Ganymede's aurora on the flow facing side of the moon is the Jovian plasma penetrating through the cusps above the separatrix, while the main source of electrons generating the aurora on the magnetotail side of Ganymede is the magnetospheric plasma penetrating Ganymede's ionosphere at latitudes below the separatrix. Figure 11 further shows that the auroral emissions exhibit different morphologies and brightnesses between the Northern and the Southern hemispheres of Ganymede. The Jovian flow facing side observation reveals that the brightest emissions are located at latitudes higher in the Northern hemisphere than in the Southern hemisphere. On the contrary, it can be noticed that on the magnetotail side view of Ganymede's aurora, the brightest emissions are located at lower latitudes in the Northern hemisphere compared to the Southern hemisphere. Finally, it is worth noticing from Figure 11 that, similar to the aurora at Earth, the auroral emissions at Ganymede tend to organize in an oval circling the Polar Regions, with nevertheless some very faint emissions between the Jovian flow facing side aurora and the magnetotail side aurora. The oval appears to be compressed to large latitudes on the Jovian flow facing side and to be extended to lower latitudes on the magnetotail side. This is consistent with the strong electrodynamic interaction of Ganymede's magnetosphere with the Jovian plasma

flowing past it which compresses Ganymede's magnetosphere in the upstream direction and stretches it in the downstream direction, thus mimicking the interaction of the Solar Wind with the Earth's magnetosphere.

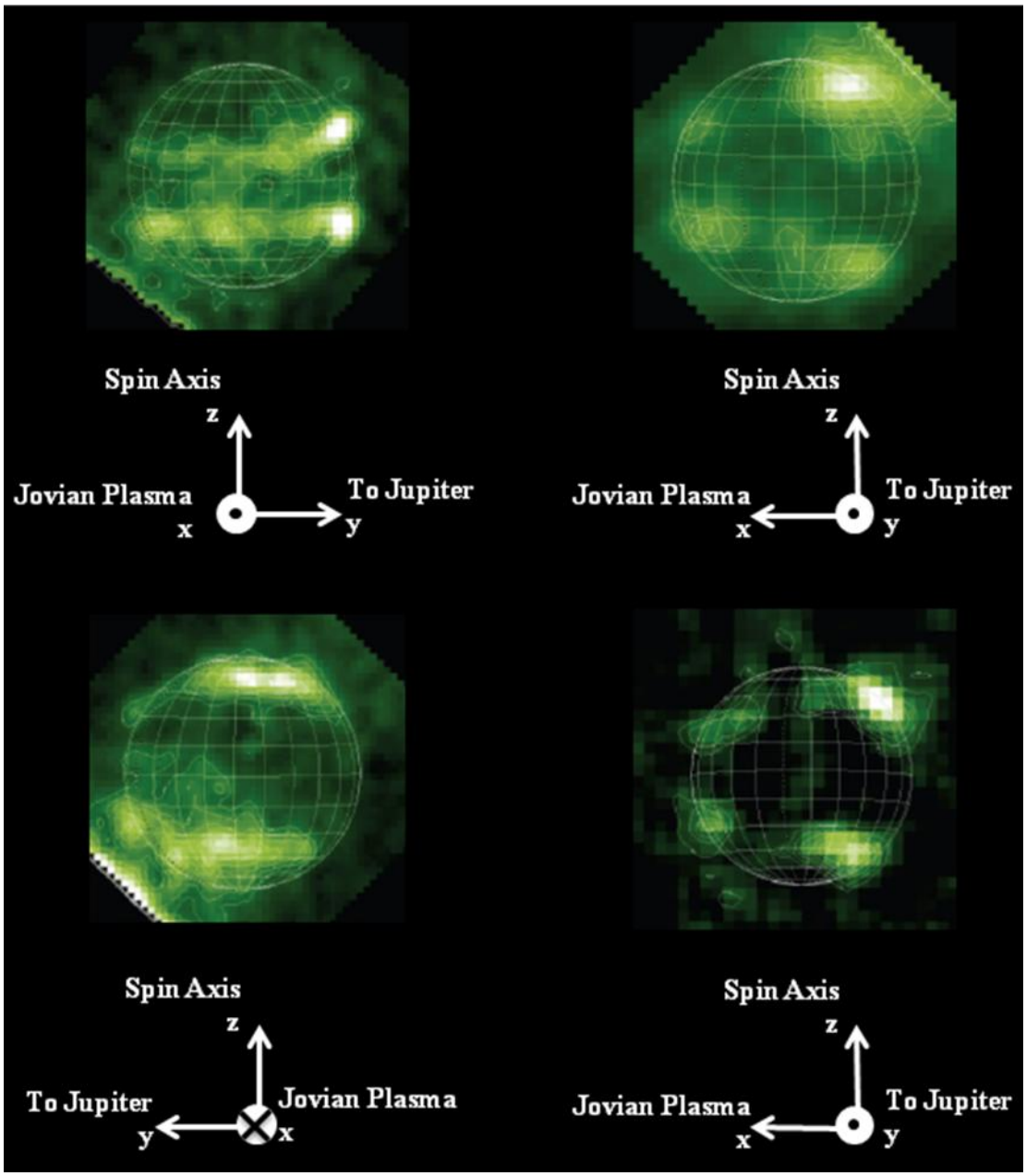

Figure 11: Ganymede's Aurora on the Magnetotail Side (Upper Left Image), on the Jovian Flow Facing Side (Lower Left Image) and on the Jovian Facing Side (Two Images to the Right) (Adapted From [*Retherford*, 2009; *McGrath et al.*, 2013])

The aurora at Ganymede is most probably produced by dissociative impact excitation of atmospheric O_2 molecules from precipitating electrons. The observed brightness of Ganymede's auroral footprint at Jupiter (order of tens of kilorayleighs) [*Clarke et al.*, 2002] confirms the strong interaction between Ganymede's magnetosphere and the corotating Jovian magnetospheric plasma. In particular, [*Frank et al.*, 1997] reported that, as the Galileo spacecraft traversed Ganymede's Polar Regions, it detected strong ionospheric outflows of H^+ and O^+ ions. These outflows of ions from Ganymede's ionosphere actually balance the inflow of Jovian magnetospheric particles due to reconnection of Ganymede's magnetic field with Jupiter's magnetic field and responsible for the generation of the Jovian flow facing side aurora at Ganymede.

3.1.2. Modeling Ganymede's Magnetosphere

In order to fully understand the plasma environment of Ganymede and its magnetic signatures, it is necessary to account for Ganymede's ionospheric composition and density. This implies being able to discriminate the different sources of ions in the near-Ganymede plasma environment. Several researchers have used resistive MHD to study the effects of variations in the incident Jovian magnetic field configuration on Ganymede's magnetospheric and ionospheric processes [*Kopp and Ip*, 2002; *Ip and Kopp*, 2002; *Jia et al.*, 2008, 2009]. In this approximation, all length-scales of variations are required to be longer than the ion gyroradius such that the associated ion drift motions, resulting from diffusion of the magnetic field through the ion plasma fluid, are negligible. However, this is not the case at Ganymede, where the gyroradius of the major component ion (O^+) can vary from 400 km in the incident Jovian plasma flow to many thousands of kilometers near reconnection regions where the magnetic field becomes very weak [*Neubauer*, 1998]. In this case, the ion gyroradius is larger than relevant

length-scales, mainly the height of the ionosphere (125 km), Ganymede's radius (2,634 km), and the altitude of the magnetopause above Ganymede's surface (2236-4788 km) [*Paty and Winglee*, 2006]. Hence, the very fact that the near-space environment of Ganymede is populated by several ion species with large gyroradii traveling in weak magnetic fields invalidates a general assumption of the ideal MHD and of the resistive MHD. In this case, a multifluid treatment is required. In the model developed by Paty and Winglee, three main ion species are modeled: the Jovian plasma, considered a single fluid of hot and heavy ions, the magnetospheric H^+ ions, and the magnetospheric O^+ ions sourced from Ganymede's magnetotail.

3.2. Brightness Model

As the Jovian plasma sources and the Ganymede's magnetospheric plasma sources precipitate into Ganymede's ionosphere, they collide with oxygen molecules and excite oxygen atoms according to the reaction of electron impact dissociative excitation described in (1).

$$O_2 + e^- \rightarrow O^* + O + e^- \rightarrow O + h\nu + O + e^- \tag{1}$$

The excited oxygen atoms O* then produce emissions at λ = 135.6 nm corresponding to the optically forbidden transition $3s^5S^0 \rightarrow 2p^4$ 3P. Such a transition requires the impacting electrons to have energies above the threshold energy of 14.3 eV. Moreover, the efficiency of the reaction in (1) is characterized by a collisional excitation rate (cm^3/s) [*Osterbrock*, 1898; *Retherford*, 2002] that may be estimated by (2).

$$C(T_e) = 8.0104 * 10^{-8} \frac{\sigma(T_e) kT_e}{\pi a_0^2 \sqrt{kT_e}} e^{-\frac{E}{kT_e}} \tag{2}$$

In (2), $\sigma(T_e)$ is the cross section of electron impact dissociation of O_2 (cm^2), which depends on the impacting electron temperature T_e (eV), E is the transition threshold energy, E = 14.3 eV, and a_0 is Bohr's radius ($a_0 = 5.29*10^{-9}$ cm). Table 3 in [*Kanik et al.*, 2003] provides lab measurements of absolute cross sections of electron impact dissociation of O_2 for OI] λ 1356 ($3s^5S^0 \rightarrow 2p^3P$; λ 1356 A°) expressed for electron energies ranging from 14.3 eV to 600 eV.

Using the absolute cross sections from [*Kanik et al.*, 2003], a curve fitting allows us to define an analytical relationship between the impacting electrons and the corresponding collisional excitation rate, which can then be used to calculate the resulting auroral brightness according to (3).

$$B = 10^{-6} n_e C(T_e) N(O_2) \tag{3}$$

In (3), B is expressed in Rayleighs (R), n_e is the impacting electron number density (cm^{-3}), $C(T_e)$ is the collisional excitation rate (cm^3/s), and $N(O_2)$ is the atmospheric column density of molecular oxygen at Ganymede (cm^{-2}).

3.2.1. Electron Temperatures and Densities

As can be inferred from (3), the auroral brightness depends directly on the electron number density while it depends indirectly on the electron temperature through the collisional excitation rate expressed in (2). The multifluid three-dimensional model provides bulk or average energy values in the keV range for the magnetospheric plasma sources and in the 10's of keV range for the Jovian plasma sources. This yield collisional excitation rates on the order of 10^{-9} to 10^{-8} cm^3/s. The temperatures of the two main sources of electrons generating Ganymede's aurora (Jovian plasma and magnetospheric plasma) are depicted in Figure 12 for the corresponding ion species.

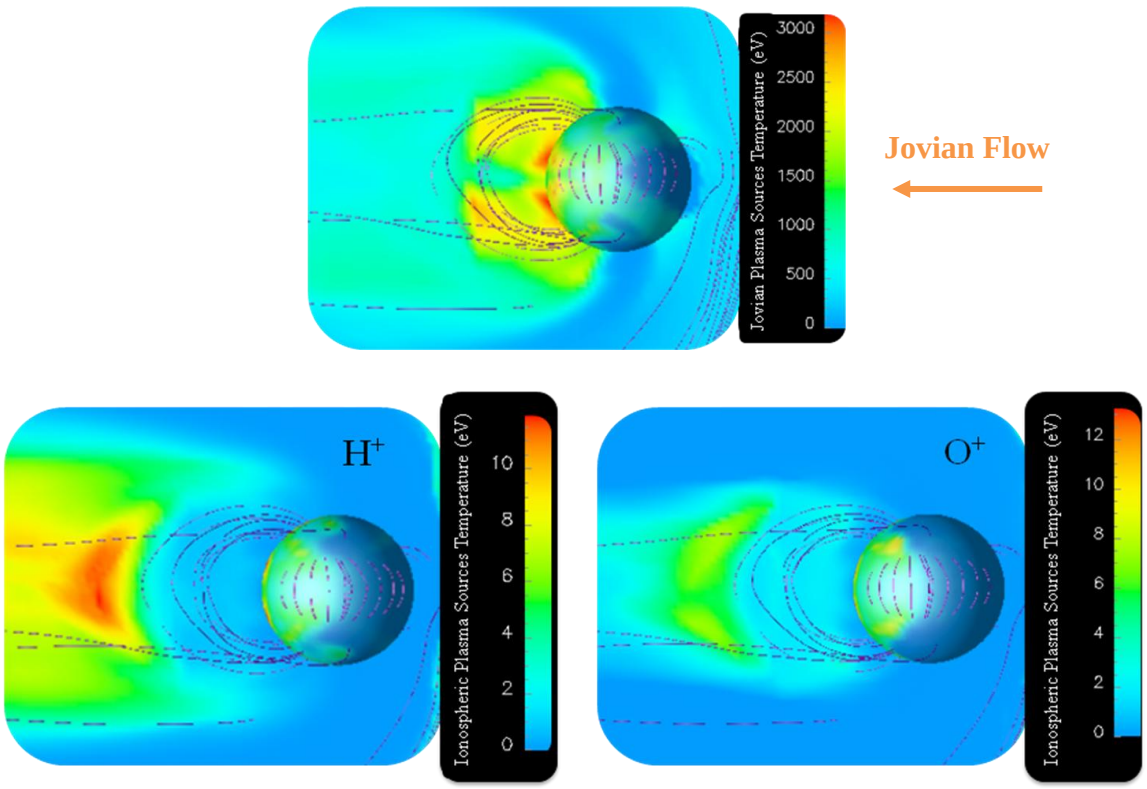

Figure 12: Energy of the Various Plasma Sources Responsible for the Generation of the Aurora at Ganymede, Provided by the Three-Dimensional Multifluid Model of Paty and Winglee [*Paty and Winglee*, 2004]

The multifluid three-dimensional model further provides bulk or average number densities ranging from 1 cm^{-3} to 10^4 cm^{-3} for the magnetospheric plasma sources, and from 1 cm^{-3} to 10 cm^{-3} for the Jovian plasma sources as shown in Figure 13. As a consequence, the electron number density has a much higher impact on the brightness value than the electron energy for a given atmospheric column density of oxygen.

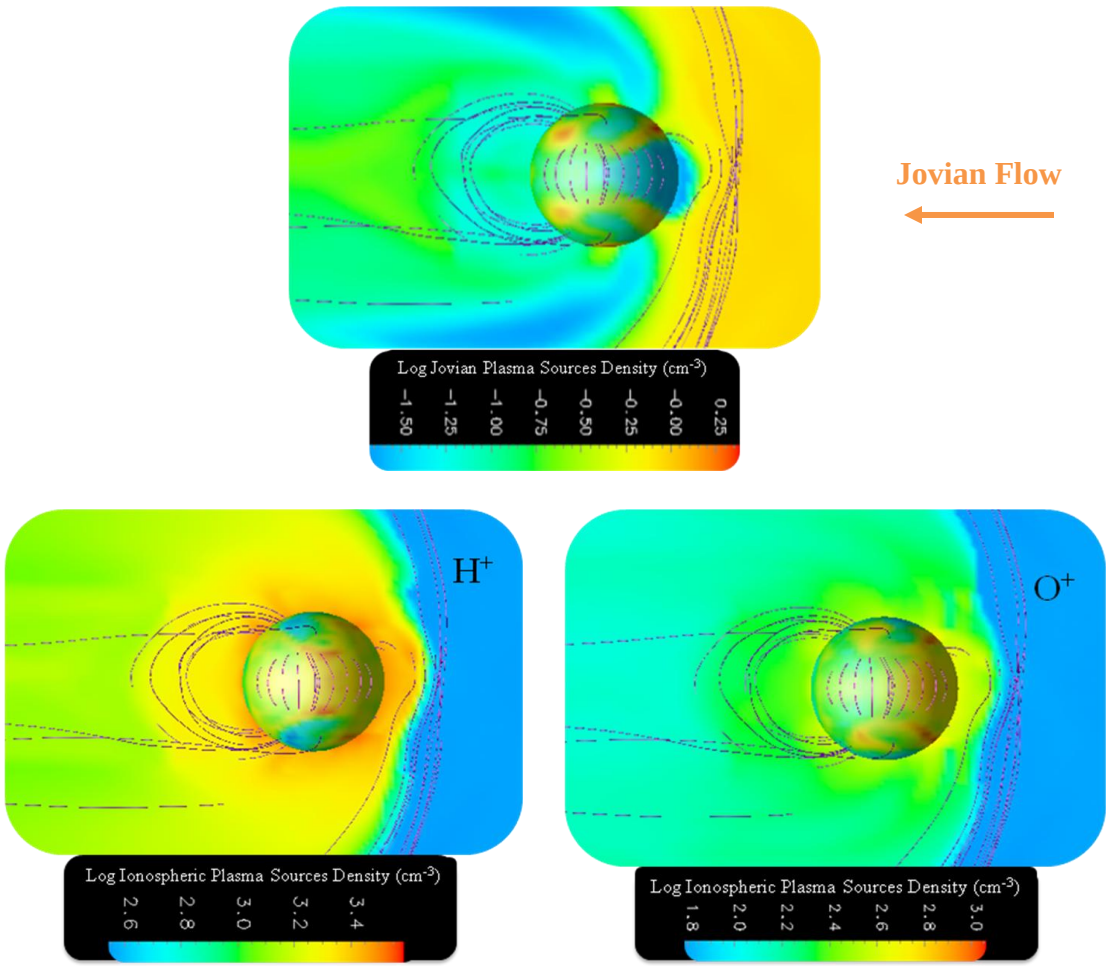

Figure 13: Number Density of the Various Plasma Sources Responsible for the Generation of the Aurora at Ganymede, Provided by the Three-Dimensional Multifluid Model of Paty and Winglee [*Paty and Winglee*, 2004]

As mentioned in section 2.1., the three-dimensional multifluid model has been validated against Galileo magnetometer data for all three positions of Ganymede with respect to the Jovian plasma sheet. Therefore, it is legitimate to assume that the average electron number densities and electron temperatures provided by the model at the locations of Ganymede where the aurora is generated is representative of the actual Jovian and magnetospheric plasma properties.

3.2.2. Atmospheric Column Density

As can be inferred from (3), the auroral brightness depends directly on the atmospheric column density of molecular oxygen at Ganymede $N(O_2)$. In this study, the number densities and temperatures of the electrons generating the aurora at Ganymede are provided by the three-dimensional multifluid model, and are assumed to realistically describe the actual Jovian and magnetospheric plasma characteristics at the locations where the auroral emissions are observed.

In order for the brightness model to be able to predict auroral brightnesses that are in agreement with observations of the aurora at Ganymede, it is therefore necessary to select carefully the value of $N(O_2)$ that ought to be used.

In previous studies, the atmospheric column density of molecular oxygen $N(O_2)$ at Ganymede was derived from a suite of measurements and observations of the aurora that were taken from different spacecraft following different trajectories at a distance from Ganymede. In other words, $N(O_2)$ was not measured directly but rather inferred from combined measurements that were not collocated in time or space, and that were taken at a distance from the moon, far away from where the aurora is actually generated. For instance, using a combination of measurements and observations from the Hubble Space Telescope (HST), the Voyager 1 spacecraft, and the Galileo spacecraft, it was obtained that Ganymede has a tenuous atmosphere of molecular and atomic oxygen, with column densities varying between about 10^{13} cm^{-2} near the Polar Regions and 10^{15} cm^{-2} near the equatorial regions [*Feldman et al.*, 2000; *Eviatar et al.*, 2001]. In this case, the Hubble Space Telescope (HST) measured the O I] λ1356 brightness of Ganymede's northern polar cap, the Voyager 1 spectrometer observed the optical depth of the far-UV absorption through radio-occultation, and the Galileo spacecraft measured the electron distribution at Ganymede.

In addition, Hall et al. estimated that near the Polar Region, above 45° latitude, and for molecular oxygen atmospheric scale heights ranging from 100 km to 1000 km, the upper limit on $N(O_2)$ must range between $5*10^{14}$ cm^{-2} and 10^{15} cm^{-2}. Assuming an electron number density of 100 cm^{-3} and a Jovian electron temperature of 120 eV, the analysis further indicated that near the Polar Regions, the lower limit on $N(O_2)$ needed to range between 10^{14} cm^{-2} and 10^{15} cm^{-2}. Nevertheless, in this study, both the electron number density and the electron temperature were measured at a distance from Ganymede, and not where the aurora is actually generated. This, combined with poor constraints on the electron distribution, makes it impossible to determine the actual plasma conditions at the locations where the auroral emissions are observed, and introduces a large amount of uncertainty in the estimated values for $N(O_2)$ [*Hall et al.*, 1998]. Eviatar et al. later reviewed the values of the atmospheric column density of molecular oxygen provided by Hall et al. Assuming a molecular oxygen scale height of 21.5 km in the region poleward of 45° latitude, they derived that $N(O_2)$ should be close to $7.4*10^{12}$ cm^{-2} near the Polar Regions. In the closed field lines region, at latitudes smaller than the separatrix (< 45°), they showed that N(O) is about $3*10^{14}$ cm^{-2} for an atmospheric scale height of 54 km [*Eviatar et al.*, 2001]. This information may be used to determine an approximate value of $N(O_2)$ in the closed field lines region of about $6*10^{14}$ cm^{-2}. Finally, Feldman et al. constructed a model atmosphere of Ganymede to derive the brightness of the auroral emissions in the open field line region. Assuming Jovian electron temperatures between 4 eV and 20 eV, they showed that $N(O_2)$ ranges from $0.3*10^{14}$ cm^{-2} to $5.2*10^{14}$ cm^{-2}. With this, they obtained brightnesses in the range of 300 R and showed that the polar limb brightening was close to 1 kR [*Feldman et al.*, 2000].

All the aforementioned studies confirm that the actual value of the atmospheric column density of molecular oxygen $N(O_2)$ near the Polar Regions is significantly uncertain. Indeed, the lack of knowledge of the distribution functions of the precipitating electrons generating the aurora and of the associated fluxes makes it impossible to

accurately derive $N(O_2)$ from the HST images of Ganymede's aurora. However, the three-dimensional multifluid model used in this study has the advantage that it provides average electron number densities and temperatures at Ganymede where the aurora is actually generated (cf. section 2.1. and 3.2.1.). In this work, an atmospheric column density $N(O_2) \sim 3.75*10^{14}$ cm^{-2} has been implemented to calculate the brightness of the auroral emissions on the Jovian flow facing side of the moon. The resulting brightness values and their comparison with observations of Ganymede's aurora from the HST provided in Figure 10 and Figure 11 may then be used to check the validity of this assumption, and potentially refine the value of $N(O_2)$ near the Polar Regions.

Observations of the magnetotail side aurora at Ganymede being very scarce, it is trickier to determine an adequate value for the atmospheric column density of molecular oxygen when calculating the brightness of the magnetotail side aurora generated by magnetospheric electrons originating from reconnection processes in Ganymede's magnetotail. In this case, since the magnetospheric plasma sources precipitate into Ganymede's ionosphere at latitudes below the separatrix, it seems appropriate to consider the atmospheric column density of molecular oxygen in the closed field lines region to calculate the brightness of the magnetotail side auroral emissions. Nevertheless, once again, it is not possible to accurately derive $N(O_2)$ from the HST images of Ganymede's aurora due to the lack of knowledge of the distribution functions of the precipitating electrons generating the aurora and the associated fluxes.

In the close field lines region, the atmospheric column density of molecular oxygen $N(O_2)$ averages $5*10^{14}$ cm^{-2}. Given that the magnetotail side aurora is located between 10° and 20° latitudes, interpolating the atmospheric column density of molecular oxygen between the Polar Regions (where $N(O_2) \sim 3*10^{13}$ cm^{-2}) and the closed field lines region near the equator (where $N(O_2) \sim 5*10^{14}$ cm^{-2}) corresponds to an atmospheric column density of molecular oxygen $N(O_2)$ of about 10^{14} cm^{-2}. Taking into account the uncertainty in the average magnetospheric electron temperatures, a value of $N(O_2) \sim 10^{13}$

cm^{-2} has been implemented in the brightness model to calculate the brightness of the magnetotail side aurora of the moon. Once again, one may check the accuracy of this assumption by comparing the brightness values provided by the brightness model with observations of Ganymede's aurora from the HST provided in Figure 11.

3.2.3. Auroral Brightness Calculation

As mentioned by Paty and Winglee [*Paty and Winglee*, 2004], the three-dimensional multifluid model provides bulk or average properties of the plasma species, from which the average electron properties may be derived. In addition, in order to excite the aurora at Ganymede through dissociative impact excitation of oxygen molecules, the precipitating electrons need to have bulk energies larger than the excitation threshold of 14.3 eV. However, as depicted in Figure 12, a majority of the modeled bulk energies of the cold magnetospheric plasma species originating from Ganymede's magnetotail fall under 14.3 eV. Therefore, only the fraction of the cold magnetospheric plasma having an average energy larger than 14.3 eV and precipitating into Ganymede's ionosphere is actually generating auroral emissions. On the contrary, the hot Jovian plasma species have modeled bulk energies well above the excitation threshold and about 300 times larger than those of the cold ionospheric plasma species. Therefore, a large majority if not all of the hot Jovian plasma precipitating into Ganymede's ionosphere through the cusps is able to excite the aurora. If one assumes that the energy of each plasma species follows a Maxwell-Boltzmann distribution centered at its average modeled energy, then the fraction of plasma species having an energy larger than the excitation threshold may be determined by an energy integration, as illustrated notionally in blue in Figure 14 and as done in (4).

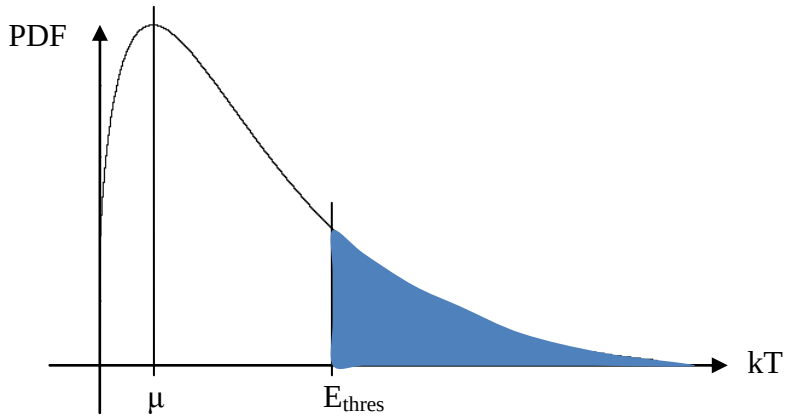

Figure 14: Maxwell-Boltzmann Distribution of the Energy of Plasma Species *s* and Integration of the Fraction of Plasma Species *s* Having an Energy Above the Excitation Threshold Energy E_{thres}

$$F_s = \sqrt{\frac{2}{\pi}} \int_{E_{thres}}^{\infty} \frac{x^2 e^{-\frac{x^2}{2a^2}}}{a^3} dx = 1 - \operatorname{erf}\left(\frac{E_{thres}}{\sqrt{2}a}\right) + \frac{1}{a} E_{thres} \sqrt{\frac{2}{\pi}} e^{-\frac{E_{thres}^2}{2a^2}}$$

$$a = \frac{\mu}{2}\sqrt{\frac{2}{\pi}}$$

(4)

In (4), F_s is the fraction of plasma species *s* that has an energy above the excitation threshold, E_{thres} is the excitation threshold (E_{thres} = 14.3 eV), and μ is the bulk temperature (eV). However, given that the collisional excitation rate is a function of the temperatures of the plasma species, it is necessary to consider a piecewise integration of the Maxwell-Boltzmann energy distribution above the excitation threshold up to the maximum bulk energy of the plasma species considered (a few keV for the magnetospheric plasma sources and some 10's of keV for the Jovian plasma sources). The lower bound of integration for each piece, named $E_{min} = kT_{e\_min}$ (where k is the Plank's constant k = $6.626*10^{-34}$ $m^2.kg.s^{-1}$), then varies from 14.3 eV to the maximum bulk energy of the plasma species considered minus one step of integration. As for the upper bound of integration, called $E_{max} = kT_{e\_max}$, it varies from 14.3 eV plus one step of

integration to the maximum bulk energy of the plasma species considered. This way, one may determine the fraction of plasma species that has an energy between E_{min} and E_{max}. Step *i* of the piecewise Maxwell-Boltzmann integration between a minimum energy E_{min_i} and a maximum energy E_{max_i} is illustrated notionally in Figure 15 and is performed using (5).

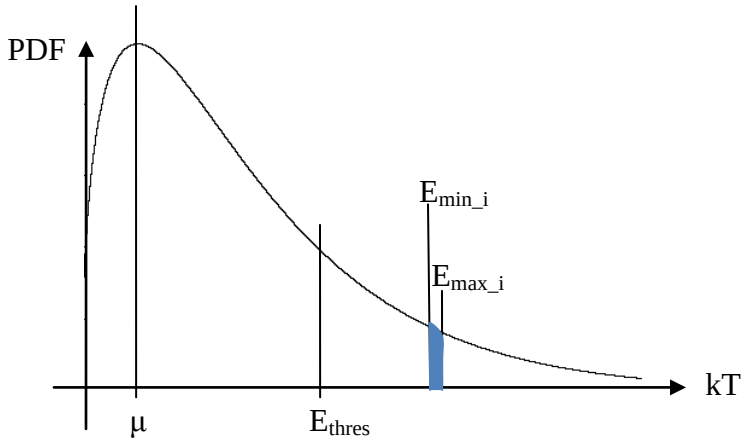

Figure 15: Integration of the Fraction of Plasma Species *s* Which has an Energy Between a Minimum Energy E_{min_i} and a Maximum Energy E_{max_i}

$$F_{s\_i} = \sqrt{\frac{2}{\pi}} \int_{E_{min\_i}}^{E_{max\_i}} \frac{x^2 e^{-\frac{x^2}{2a^2}}}{a^3} dx = \operatorname{erf}\left(\frac{E_{max\_i}}{\sqrt{2}a}\right) - \operatorname{erf}\left(\frac{E_{min\_i}}{\sqrt{2}a}\right) + \frac{1}{a} E_{max\_i} \sqrt{\frac{2}{\pi}} e^{-\frac{E_{max\_i}^2}{2a^2}} - \frac{1}{a} E_{min\_i} \sqrt{\frac{2}{\pi}} e^{-\frac{E_{min\_i}^2}{2a^2}} \quad (5)$$

In (5), F_{s_i} is the fraction of plasma species *s* that has an energy between E_{min_i} and E_{max_i}, E_{thres} is the excitation threshold (E_{thres} = 14.3 eV), and μ is the bulk temperature (eV). At each step of integration, the minimum energy is used to calculate the corresponding collisional excitation rate. The auroral brightness at step *i* can then be derived from (6).

$$B_i = B_{i-1} + 10^{-6} F_{s\_i} n_e C_i(T_{e\_min}) N(O_2) \quad (6)$$

In (6), B_{i-1} is the auroral brightness at step *i-1* expressed in Rayleighs, $F_{s\_i}*n_e$ is the fraction number density of impacting electrons having an energy between E_{min_i} and E_{max_i} (cm^{-3}), $C_i(T_e)$ is the corresponding collisional excitation rate calculated from the lower energy bound (cm^3/s), and $N(O_2)$ is the atmospheric column density of molecular oxygen in Ganymede's atmosphere (cm^{-2}).

3.2.4. Parallel Electric Field Calculation

As mentioned previously, magnetic reconnections in Ganymede's magnetotail are responsible for the generation of acceleration regions through which magnetospheric plasma sources may gain energy and precipitate into Ganymede's ionosphere to produce the aurora. Such acceleration regions correspond to enhanced parallel electric fields along the magnetic field lines of Ganymede. In order to get insight into the potential correlation between the regions of magnetospheric plasma acceleration and the regions of brightest auroral emissions, one may derive the parallel electric fields from the Generalized Ohm's Law as described in (7).

$$\vec{E} = -\sum_s \frac{n_s \vec{v}_s \times \vec{B}}{n_e} + \frac{\vec{j} \times \vec{B}}{n_e e} - \frac{\nabla P_e}{n_e e}$$

$$\Rightarrow \mathrm{E}_{\parallel} = -\frac{\vec{\mathrm{E}} \bullet \vec{\mathrm{B}}}{\left\| \vec{\mathrm{B}} \right\|} \qquad (7)$$

In (7), n_s is the number density of species *s* (cm^{-3}), n_e is the electron number density (cm^{-3}), $\vec{j}$ is the total electromagnetic current density ($A.m^{-2}$), P_e is the electron pressure, $\vec{v}_s$ is the velocity of species *s* ($m.s^{-1}$), $\vec{B}$ is the magnetic field (T), $\vec{E}$ is the electric field (A), and e is the elementary charge ($1.6*10^{-19}$ C).

While previous studies have mainly focused on determining current systems as a proxy to study acceleration structures in the vicinity of Ganymede, the three-dimensional multifluid model used in this study provides the capability to directly and accurately calculate the parallel electric fields from the Generalized Ohm's Law. This is because most studies of Ganymede's magnetosphere have involved Magnetohydrodynamics models [*Jia et al.*, 2008; *Jia et al.*, 2009]. However, MHD models are not valid in the presence of strong currents parallel to the magnetic field. In such cases, it is essential to introduce the effects of the electron thermal gradient and of the collisional resistivity of the plasma in the Generalized Ohm's Law through the terms $-\frac{\nabla P_e}{n_e e}$ and $\eta\vec{j}$ respectively.

3.2.5. Field-Aligned Current Density Calculation

In order to visualize the transition between open and closed magnetic field lines or separatrix, and to analyze the correlation between the corresponding latitudes and the morphology of the aurora at Ganymede, the field-aligned current density may be determined using (8):

$$j_{\parallel} = \frac{\vec{j} \bullet \vec{B}}{\left\|\vec{B}\right\|} \tag{8}$$

CHAPTER 4

MODELING RESULTS

4.1. Case Studies

The brightness model described above and the parallel electric field calculations have been applied to three different upstream Jovian plasma conditions corresponding to three different positions of Ganymede with respect to the center of the Jovian plasma sheet, as summarized in Table 1.

Table 1: Case Studies for the Brightness Model

Position of Ganymede relative to the Jovian plasma sheet	Flow speed (km/s)	Bx (nT)	By (nT)	Bz (nT)
ABOVE	180	17	-73	-85
CENTER	180	-11	11	-77
BELOW	180	-7	78	-76

4.2. Long-Period Variability Study

The long-period variability described for Ganymede footprint by Grodent et al. [*Grodent et al.*, 2009] at Jupiter may be observed in the morphology and brightness of Ganymede's aurora for different positions of the moon with respect to the center of the Jovian plasma sheet. Table 2 depicts Ganymede's aurora on the Jovian flow facing side and on the Ganymede's magnetotail side, and compares it to the corresponding HST/STIS image published by [*Feldman et al.*, 2000]. Table 3 shows the corresponding regions of enhanced parallel electric fields corresponding to regions of accelerations of Jovian and magnetospheric plasma sources. It may be noticed that these regions of acceleration correlate rather well with the regions of brightest auroral emissions.

Table 2: Long-Period Variability Study

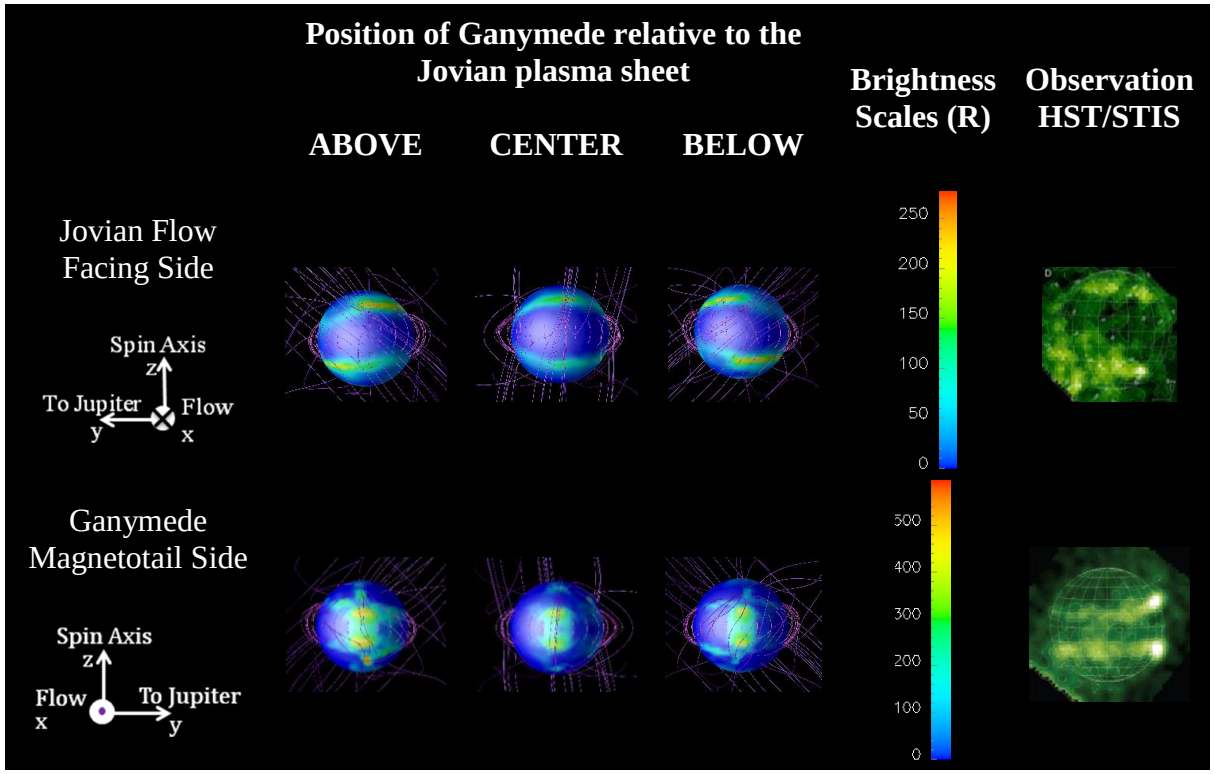

Table 3: Parallel Electric Fields and Acceleration Regions

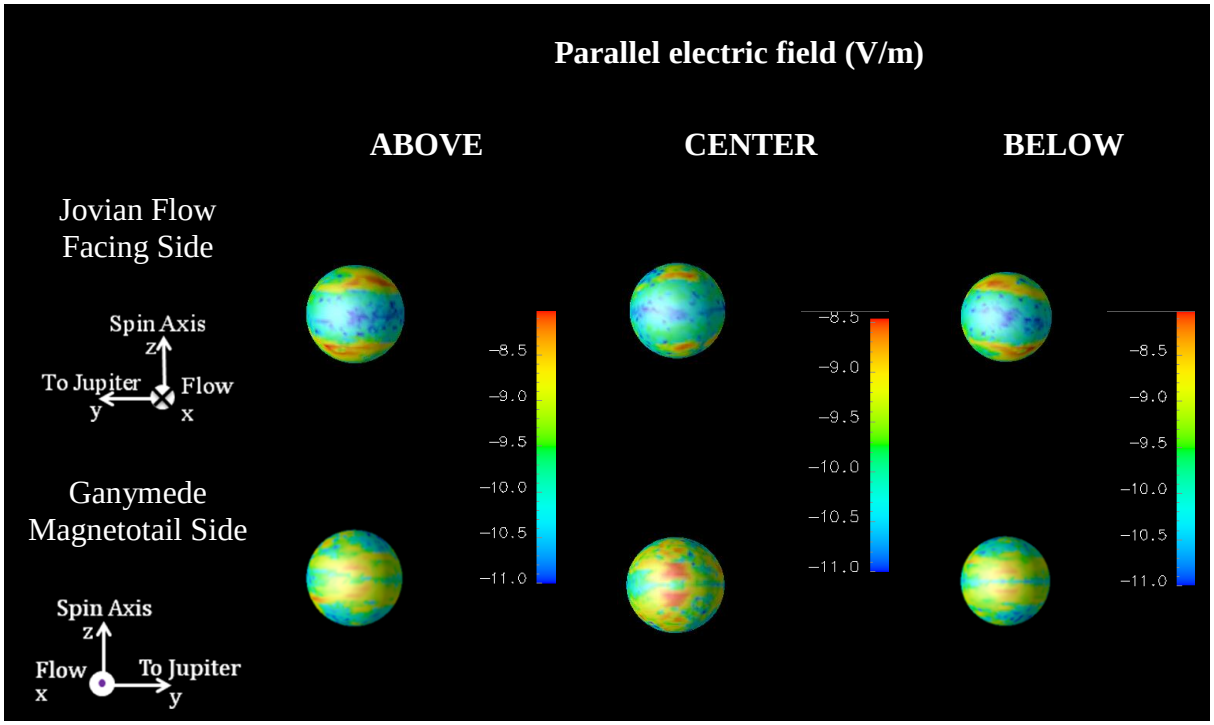

4.3. Short-Period Variability Study

The short-period variability described for Ganymede footprint by Grodent et al. [*Grodent et al.*, 2009] at Jupiter may be observed in the morphology and brightness of Ganymede's aurora for a given position of the moon with respect to the center of the Jovian plasma sheet. Table 4 depicts Ganymede's aurora on the Jovian flow facing side and on the Ganymede's magnetotail side, for three consecutive times. The time interval between each figure in Table 4 is 140 second as obtained after treatment of the output from the three-dimensional multifluid model. Table 4 also shows the corresponding regions of enhanced parallel electric fields corresponding to regions of accelerations of Jovian and magnetospheric plasma sources. These regions of acceleration correlate rather well with the regions of brightest auroral emissions. Figure 16 compares the morphology of the aurora at Ganymede obtained from the brightness model when observed from Jupiter, with that observed by the HST/ACS-SBC [*McGrath et al.*, 2013]. On the figure to the right of Figure 16, brightness contours are in Rayleighs (R), and vary from 100 R to 300 R for the brightest emissions.

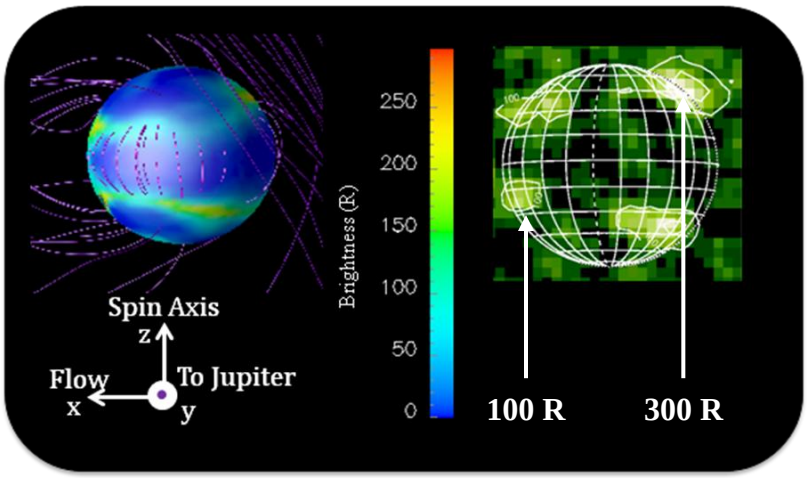

Figure 16: Comparison of the Morphology of Ganymede's Aurora Provided by the Brightness Model With the Corresponding Observation by the HST/ACS-SBC ([*McGrath et al.*, 2013])

Table 4: Short-Period Variability Study

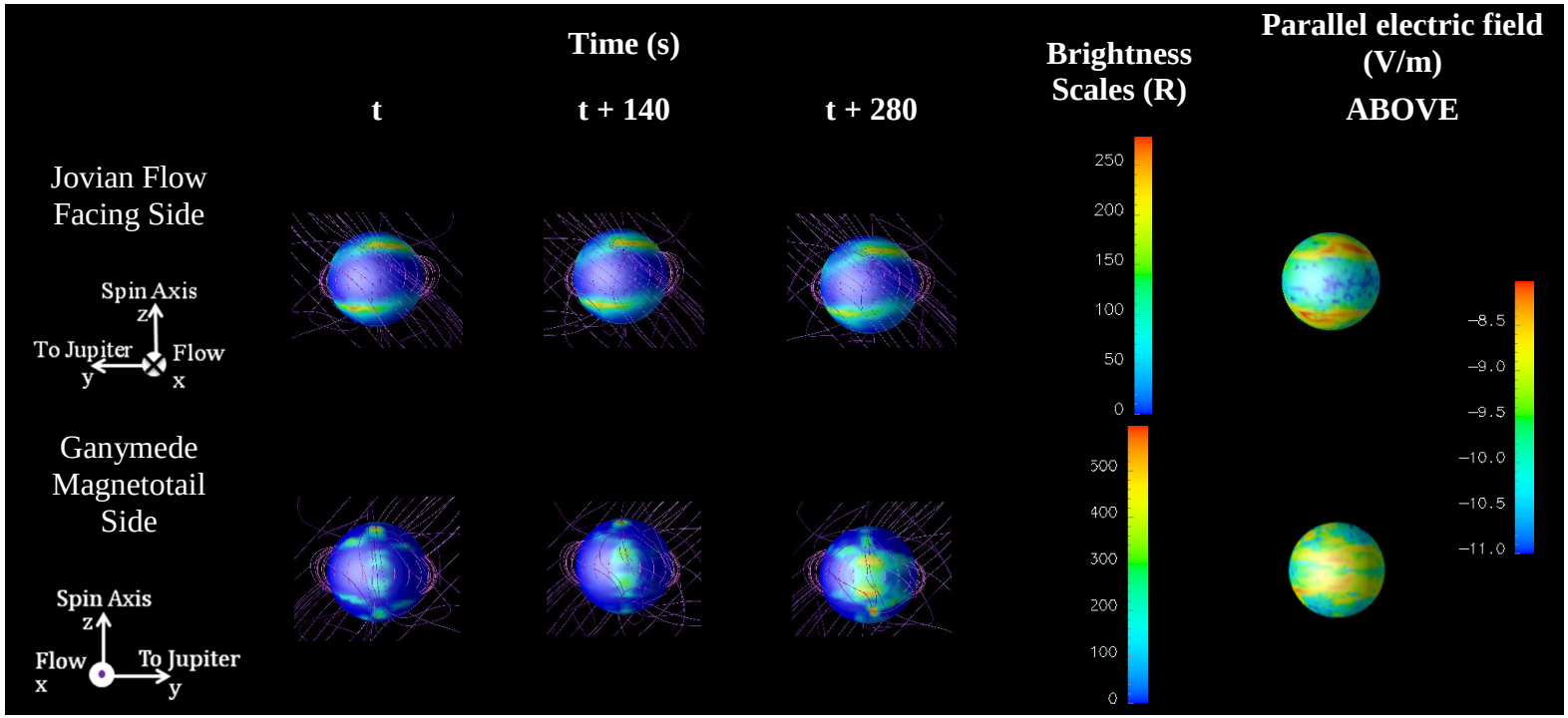

4.4. Visualization of the Separatrix Region – Filed-Aligned Currents

The field-aligned currents provide a way to visualize the transition from open field lines near the Polar Regions to closed field lines closer to the equator, or separatrix. Table 5 provides various views of the field-aligned current systems at Ganymede.

Table 5: Field-Aligned Currents at Ganymede

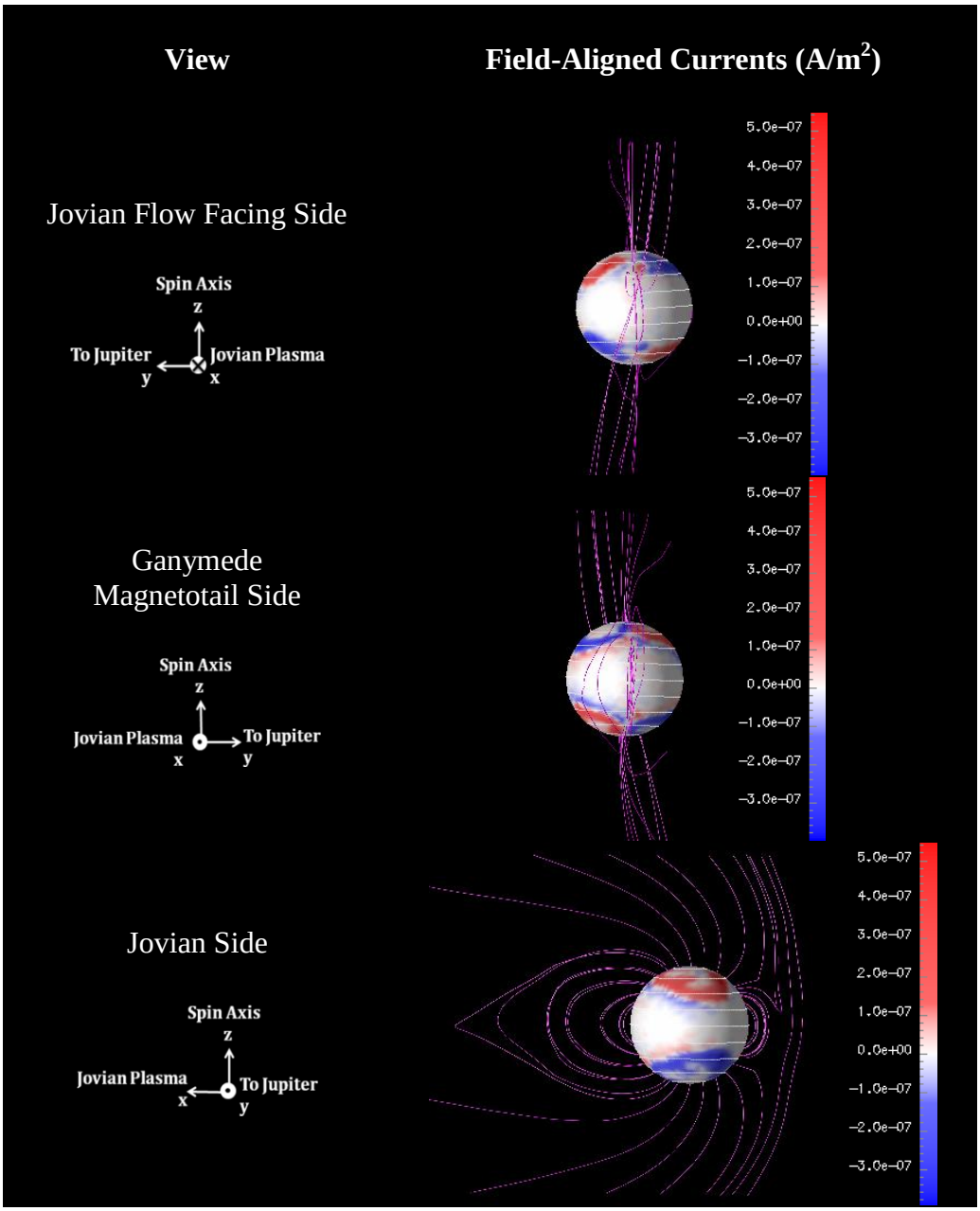

Table 5: Field-Aligned Currents at Ganymede (Continued)

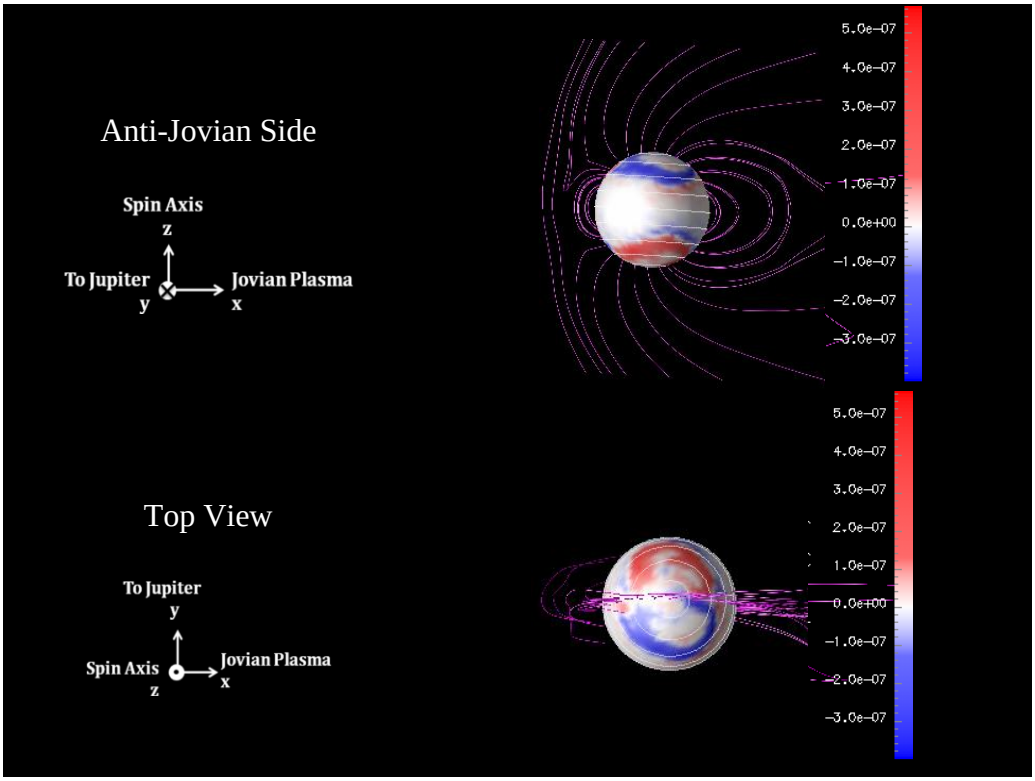

From Table 5, one may notice that the field-aligned currents reflect the convection pattern in Ganymede's magnetosphere. First, the open magnetic field lines on the Jovian flow facing side of Ganymede reconnect with the Jovian magnetic field lines on Ganymede's magnetopause. Then, the newly reconnected magnetic field lines convect to Ganymede's magnetotail. As the Jovian plasma flows around Ganymede's magnetosphere, magnetic pressure builds up and pushes the convecting magnetic field lines against each other until they reconnect. Finally, the closed magnetic field lines reconnected in Ganymede's magnetotail convect back towards the moon as they release the energy acquired through reconnection. This Dungey-like cycle is clearly identifiable from the top view of the field-aligned currents provided in Table 5 where it presents a bean-like shape. In addition, Table 5 shows that on the Jovian side of Ganymede, the field-aligned currents traveling along the open field lines convecting downward to Ganymede's magnetotail are outflowing in the Northern hemisphere and inflowing

towards the moon in the southern hemisphere. These field-aligned currents flowing along open field lines are similar to the Region 1 currents in the Earth's magnetosphere. A pair of field-aligned currents with opposite polarities is found at lower latitudes. These field-aligned currents travel along the closed field lines generated by reconnection processes in Ganymede's magnetotail that convect back to the moon. These field-aligned currents flowing along closed field lines are similar to the Region 2 currents in the Earth's magnetosphere. Finally, on the anti-Jovian side of Ganymede, the polarities are all reversed between the northern and the southern hemispheres of Ganymede.

On the figures in Table 5, the white horizontal lines on Ganymede's surface represent latitude lines, each spaced 15° apart. Then, one may infer that the separatrix region between the open and closed magnetic field lines is located around 30-45° latitude. This is consistent with observations and calculations of the latitudinal location of the separatrix from Feldman et al. [*Feldman et al.*, 2000] and McGrath et al. [*Retherford*, 2009; *McGrath et al.*, 2013].

Observing concurrently Table 2, Table 3, Table 4, and Table 5, one may notice that the Jovian magnetic field lines reconnect to Ganymede's magnetic field lines at latitudes poleward of the separatrix region on the Jovian flow facing side of Ganymede's magnetopause. Such local reconnection processes are responsible for the creation of the aurora on the flow facing side of Ganymede where the Jovian plasma sources penetrate into Ganymede's ionosphere through the cusps, just above the separatrix region. Then, the newly reconnected open magnetic field lines convect to Ganymede's magnetotail where they reconnect one more time due to a build-up of the magnetic pressure from the Jovian plasma flowing around Ganymede's magnetosphere. These secondary local reconnection processes are responsible for the generation of acceleration regions through which Ganymede's magnetospheric plasma sources gain energy, travel along the newly reconnected closed magnetic field lines, and precipitate into Ganymede's ionosphere at latitudes well below the separatrix region to generate the magnetotail side aurora.

4.5. Discussion of the Results

As may be noticed from Table 2 and Table 4, the brightness model predicts longitudinally non-uniform auroral emissions with brightness values ranging from 100 R to 300 R on the Jovian flow facing side depending on the latitude. The brightest emissions are further confined to geomagnetic latitudes defining the boundaries of the polar caps (above 40° latitude) in both the Northern and the Southern hemispheres. This correlates well with the HST images of Ganymede's aurora shown in Figure 10 [*Feldman et al.*, 2000]. On the magnetotail side, the brightness model yields longitudinally and latitudinally non-uniform auroral emissions with slightly larger maximum auroral brightness values (~ 500 R) compared to the corresponding observation (~ 400 R as shown on the upper left image in Figure 11) [*McGrath et al.*, 2013]. In addition, the model shows that auroral emissions are brightest at higher latitudes on the Jovian flow facing side compared to the magnetotail side where the aurora is mainly located below the separatrix between 10° and 20° latitudes. This suggests that the main source of electrons generating Ganymede's aurora on the flow facing side of the moon is the Jovian plasma penetrating through the cusps above the separatrix, while the main source of electrons generating the aurora on the magnetotail side of Ganymede is the magnetospheric plasma penetrating Ganymede's ionosphere at latitudes below the separatrix.

In addition, Table 2 and Table 4 highlight that the auroral emissions exhibit different morphologies and brightnesses in the Northern and the Southern hemispheres of Ganymede. On the Jovian flow facing side, the model predicts that auroral emissions are brightest at latitudes higher in the Northern hemisphere than in the Southern hemisphere. On the contrary, on the magnetotail side view of Ganymede's aurora, the brightest emissions are located at lower latitudes in the Northern hemisphere compared to the Southern hemisphere. The model further shows that auroral emissions at Ganymede tend

to organize in an oval circling the Polar Regions, with nevertheless some very faint emissions between the Jovian flow facing side aurora and the magnetotail side aurora. The oval appears to be compressed to high latitudes on the Jovian flow facing side and to extend to lower latitudes on the magnetotail side.

Finally, Table 2, Table 3, and Table 4 show that the regions of largest parallel electric field correlate with the morphology of the aurora at Ganymede where the brightest auroral emissions coincide with the regions of electron accelerations corresponding to magnetic reconnection on the dayside and on the tail-side of Ganymede's magnetosphere.

To conclude, the morphology and brightness of Ganymede's aurora on the Jovian plasma flow facing side and on the Ganymede's magnetotail side both agree with the HST observations provided in Figure 10 and Figure 11 [*Feldman et al.,* 2000; *McGrath et al.*, 2013]. The modeled aurora at Ganymede reveals that the periodicities of the morphology and the brightness of the auroral emissions are produced by two different dynamic reconnection mechanisms. The Jovian flow facing side aurora is generated by electrons sourced in the Jovian plasma and penetrating into Ganymede's ionosphere through the cusps above the separatrix region. In this case, the reconnection processes responsible for the auroral emissions occur on Ganymede's magnetopause between the Jovian magnetic field lines and the open magnetic field lines threading Ganymede's Polar Regions. As for the magnetotail side aurora, it is generated by electrons originating from Ganymede's magnetospheric flow. These electrons are accelerated along closed magnetic field lines created by magnetic reconnection in Ganymede's magnetotail, and precipitate into Ganymede's ionosphere at much lower latitudes, below the separatrix region. In addition, results from the coupled model show that the aurora is brightest on the tail-side due to the higher densities of precipitating electrons accelerated through magnetic reconnections in Ganymede's magnetospheric tail. Nevertheless, the model predicts

brightness values that are slightly larger than the observations (cf. Figure 11 [*McGrath et al.*, 2013]). This may be a consequence of two types of limitations coming from the main building blocks of the brightness model. The first limitation concerns the three-dimensional simulation model which does not directly tracks the temperatures and number densities of the various electron sources generating Ganymede's aurora, but rather tracks the temperatures and number densities of the various ion sources and derives the corresponding electron properties. The second limitation concerns the value of the atmospheric column density of molecular oxygen at Ganymede as derived in earlier work by Hall et al., Feldman et al. and Eviatar et al. [*Hall et al.*, 1998; *Feldman et al.*, 2000; *Eviatar et al.*, 2001]. In these studies, the atmospheric column density of molecular oxygen at Ganymede was inferred from various sources of information that were not coincident in time and space. The electrons number densities and temperatures were measured at a distance from Ganymede, while the auroral brightness values observed and used to derive $N(O_2)$ were the result of local processes occurring at Ganymede. In this context, Hall et al. admitted that the poor constraints and the lack of knowledge on the distribution functions of the precipitating electrons generating the aurora and of the associated fluxes made it impossible to accurately derive $N(O_2)$ from the HST images of Ganymede's aurora and introduced a large amount of uncertainty in the estimated values for $N(O_2)$. Nevertheless, the coupled model developed in this research provides a way to better constrain the value of the atmospheric column density of molecular oxygen at Ganymede, both near the Polar Regions and at lower latitudes. Indeed, the electron properties used by the brightness model to calculate the brightness of the auroral emissions are obtained from the three-dimensional multifluid simulation model which provides them at the locations where the Jovian side aurora and the magnetotail side aurora are generated. In this context, it was shown that the modeled auroral brightness values were consistent with the observations from the HST both on the Jovian flow facing side and on the magnetotail side. Therefore, the assumed values of $N(O_2)$ used in

the brightness model provide accurate representations of the aurora at Ganymede and may be used as refined estimates for the atmospheric column density of O_2 at the moon, both north and south of the separatrix region. Finally, the slight discrepancy between the modeled and the observed maximum brightness values in the magnetotail side aurora at Ganymede most likely originate from a combination of the two limitations described above. Nevertheless, this discrepancy remains very small.

4.6. Conclusions and Future Work

The goal of the present work has been to examine the relationship between the longest and the shortest timescale periodicities of Ganymede's auroral footprint brightness and local processes occurring at Ganymede, using a three-dimensional multifluid model coupled to a specially developed brightness model. The three-dimensional multifluid model allowed the characterization of the interaction between Ganymede's magnetosphere and the local Jovian plasma environment by tracking the energies and fluxes of charged particles precipitating into Ganymede's atmosphere. A brightness model was then developed and coupled to the three-dimensional multifluid model to understand the dynamics of Ganymede's magnetosphere in response to varying upstream Jovian magnetospheric conditions and to the fluttering of the plasma sheet over Ganymede. The brightness model allowed investigating the range of plausible auroral electron acceleration mechanisms by accounting for the precipitating electron temperatures in the calculation of the auroral brightness under various initial conditions for plasma density, magnetic field strength and magnetic field orientation. This provided insight into the variability in the brightness and morphology of Ganymede's aurora, and enabled examining any correlation with the variability of Ganymede's auroral footprint on Jupiter's ionosphere.

First, it was shown that the auroral brightness values provided by the brightness model agree well with the HST observations of Ganymede's aurora, both on the Jovian flow facing side and on the magnetotail side.

Then, the results provided by the coupled model suggested the presence of short- and long-period variabilities in the auroral brightness at Ganymede due to local magnetic reconnection processes occurring on the magnetopause and in the magnetotail. On the Jovian flow facing side, it was shown that the Jovian plasma sources of the aurora are accelerated along open magnetic field lines and precipitate into Ganymede's ionosphere through the cusps. They generate auroral emissions that are mostly located above the separatrix at 40°+ N/S latitudes. On the magnetotail side, it was demonstrated that the ionospheric and magnetospheric plasma sources are accelerated along closed magnetic field lines and precipitate into Ganymede's ionosphere at lower latitudes. They generate auroral emissions that are mainly located below the separatrix between 10° and 20° N/S latitudes.

Finally, it was shown that the present study supports the hypothesis of a correlation between the variability of Ganymede's auroral footprint on Jupiter's ionosphere and the variability in brightness and morphology of the aurora at Ganymede.

This Master's thesis will serve as the basis for a journal paper submitted to the Space Physics edition of the Journal of Geophysical Research or Geophysical Research Letters.

Last but not least, the modeling techniques and the brightness model developed in this work may be applied to other magnetospheric systems such as the Enceladus-Saturn system. Although the interaction between Ganymede and Jupiter is unique in several ways, the modeling approach taken in this study may help uncover the processes at play in the generation of a potential aurora at Enceladus, and any possible correlation with the

brightness and structural properties of the Enceladus footprint observed at Saturn. The brightness model may also be used to determine the energy deposition in Titan's atmosphere to understand Titan's atmospheric profiles and fluxes. This may provide some insight into the similarities and major differences between the Jovian system and the Saturnian system so as to understand the global processes at play.

REFERENCES

Bagenal (1994), "Empirical model of Io plasma torus: Voyager measurements", *Journal of Geophysical Research*, Vol. 99, pp. 11,043-11,062

Bagenal (1983), "Alfvén wave Propagation in the Io Plasma Torus", *Journal of Geophysical Research*, Vol. 88, pp. 3013-3025

Bagenal, F., et al. (2004), "Jupiter: The Planet, Satellites and Magnetosphere," *Cambridge University Press*

Bagenal (2007), "The magnetosphere of Jupiter: Coupling the equator to the poles", *Journal of Atmospheric and Solar-Terrestrial Physics*, Vol. 69, pp. 387-402

Baumjohann, W., R. A. Treumann (2006), "Basic Space Plasma Physics", *Imperial College Press*, London

Bazer et al. (1963), "Geometrical Hydromagnetics", *Journal of Geophysical Research*, Vol. 68, No. 1, pp. 147 - 174

Bonfond et al.. (2008), "UV Io footprint leading spot: A key feature for understanding the UV Io footprint multiplicity?," *Geophysical Research Letters*, Vol. 35, doi: 10.1029/2007GL032418

Bonfond et al. (2012), "Auroral evidence of Io's control over the magnetosphere of Jupiter", *Geophysical Research Letters*, Vol. 39, doi: 10.1029/2011GL050253

Bonfond et al. (submitted 2012), "Evolution of the Io footprint brightness I: Far-UV observations", submitted to Planetary and Space Science

Calvert, J. (unpublished data, 2011), "Magnetohydrodynamics", available from the University of Denver, Colorado (http://mysite.du.edu/~jcalvert/phys/mhd.htm)

Clarke, J. T., et al. (2002), "Ultraviolet emissions from the magnetic footprints of Io, Ganymede and Europa on Jupiter", *Nature*, Vol. 415, pp. 997-999

Crary et al. (1997), "Coupling the plasma interaction at Io to Jupiter", *Geophysical Research Letters*, Vol. 24, No. 17, pp. 2135-2138

Drell, S. D., Foley, H. M., and Ruderman, M. A. (1965), "Drag and propulsion of large satellites in the ionosphere: An Alfvén propulsion engine in space," Journal of Geophysical Research, Vol. 70, No. 13, pp 3131-3145

Elkins-Tanton, L. T. (2006), "Jupiter and Saturn", *New York: Chelsea House*, ISBN 0-8160-5196-8

Eviatar, A., V. M. Vasyliunas, and D. A. Gurnett (2001), "The ionosphere of Ganymede", *Planetary and Space Science*, Vol. 49, No. 3-4, pp. 327-336

Feldman, P. D., M. A. McGrath, D. F. Strobel, H. W. Moos, K. D. Retherford, and B. C. Wolven (2000), "HST/STIS ultraviolet imaging of polar aurora on Ganymede", *Astrophysical Journal*, Vol. 535, pp. 1085-1090

Ferraro (1954), "On the reflection and refraction of Aflvén waves", *American Astronomical Society*, pp. 393-406

Frank, L. A., W. R. Paterson, K. L. Ackerson, and S. J. Bolton (1997), "Outflow of hydrogen ions from Ganymede", *Geophysical Research Letters*, Vol. 24, pp. 2151-2154

Gerard et al. (2006), "Morphology of the ultraviolet Io footprint emission and its control by Io's location", *Journal of Geophysical Research*, Vol. 111, doi: 10.1029/2005JA011327

Glatzmaier, G. A., and Roberts, P. H. (1995), "A three-dimensional self-consistent computer simulation of a geomagnetic field reversal," *Nature*, Vol. 377, pp. 203-209

Goertz (1980), "Io's Interaction With the Plasma Torus", *Journal of Geophysical Research*, Vol. 85, No. A6, pp. 2949-2956

Grodent, D., Bonfond, B., Radioti, A., Gerard, J.-C., Jia, X., Nichols, J. D., and Clarke, J. T. (2009), "Auroral footprint of Ganymede", *Journal of Geophysical Research*, Vol. 114, A07212, doi: 10.1029/2009JA014289

Gurnett and Goertz (1981), "Multiple Alfvén Waves Reflections Excited by Io: Origin of the Jovian Decametric Arcs", *Journal of Geophysical Research*, Vol. 86, No. A2, pp. 717-722

Gurnett, D. A., et al. (1996), "Evidence for a magnetosphere at Ganymede from plasma-wave observations by the Galileo spacecraft", *Nature*, Vol. 384, pp. 535-537

Gurnett, D. A., A. Bhattacharjee (2005), "Introduction to Plasma Physics with Space and Laboratory Applications", *Cambridge University Press*, Cambridge, United Kingdom

Hall, D. T., P. D. Feldman, M A. McGrath, and D. F. Strobel (1998), "The far-ultraviolet oxygen airglow of Europa and Ganymede", *Astrophysical Journal*, Vol. 449, pp. 475-481

Hughes, W. F., and J. A. Brighton (1999), "Schaum's Outline of Theory and Problems in Fluid Dynamics", *McGraw Hill*, 3rd edition, Schaum's outline series

Ip, W.-H., et al. (1997), "Energetic ion sputtering effects at Ganymede", *Geophysical Research Letters*, Vol. 24, No. 21, pp. 2631-2634

Ip, W.-H., and A. Kopp (2002), "Resistive MHD simulations of Ganymede's magnetosphere, 2. Birkeland currents and particle energetics", *Journal of Geophysical Research*, Vol. 107, No. A12, doi:10.1029/2001JA005072

Jia, X., R. J. Walker, M. G. Kivelson, K. K. Khurana, and J. A. Linker (2008), "Three-dimensional MHD simulations of Ganymede's magnetosphere", *Journal of Geophysical Research*, Vol. 113, No. A06212, *doi:10.1029/2007JA012748*

Jia, X., R. J. Walker, M. G. Kivelson, K. K. Khurana, and J. A. Linker (2009), "Properties of Ganymede's magnetosphere inferred from improved three-dimensional MHD simulations", *Journal of Geophysical Research*, Vol. 114, No. A09209, doi:10.1029/2009JA014375

Kanik, I., Noren, C., Makarov, O. P., Vattipalle, P., and Ajello, J. M. (2003), "Electron impact dissociative excitation of O2: 2. Absolute emission cross sections of the OI(130.4 nm) and OI(135.6 nm) lines", *Journal of Geophysical Research*, Vol. 108, No. E11, pp. 5126, doi:10.1029/2000JE001423

Kivelson, M. G., K. K. Khurana, C. T. Russell, R. J. Walker, J. Warnecke, F. V. Coroniti, C. Polanskey, D. J. Southwod, and G. Shoubert (1996), "Discovery of Ganymede's magnetic field by the Galileo spacecraft", *Nature*, Vol. 384, pp. 537-541

Kivelson, M. G., K. K. Khurana, F. V. Coroniti, S. Joy, C. T., Russell, R. J. Walker, J. Warnecke, L. Bennett, and C. Polanskey, (1997), "The magnetic field and magnetosphere of Ganymede", *Geophysical Research Letters*, Vol. 24, pp. 2153-2158

Kivelson, M. G., J. Warnecke, L. Bennett, S. Joy, K. K. Khurana, J. A. Linker, C. T. Russell, R. J. Walker, and C. Polanskey (1998), "Ganymede's magnetosphere: Magnetometer overview", *Journal of Geophysical Research*, Vol. 103, pp. 19,963-19,972

Kivelson, M. G., et al. (2002), "The permanent and inductive magnetic moments of Ganymede", *Icarus*, Vol. 157, pp. 507-522

Kivelson et al. (2004), "Magnetospheric Interactions with Satellites", *Cambridge University Press, Edited by Bagenal, Dowling, and McKinno*n

Kopp, A., and W.-H. Ip (2002), "Resistive MHD simulations of Ganymede's magnetosphere, 1. Time variabilities of the magnetic field topology", *Journal of Geophysical Research*, Vol. 107, No. A12, doi:10.1029/2001JA005071

Krupp, N., Vasyliunas, V. N., Woch, J., Lagg, A., Khurana, K. K., Kivelson, M. G., Mauk, B. H., Roelof, E. C., Williams, D. J., Krimigis, S. M., Kurth, W. S., Frank, L. A., and Paterson, W. R. (2004), "Dynamics of the Jovian Magnetosphere", *In Bagenal, F. et al., "Jupiter: The Planet, Satellites and Magnetosphere", Cambridge University Press*, ISBN 0-521-81808-7

Khurana, K. K., Vasyliunas, V. M., Mauk, B. H., Kivelson, M. G., Krupp, N., Woch, J., Lagg, A., and Kurth, W. S (2004), "The configuration of Jupiter′s Magnetosphere", Book Chapter 24, edited by F. Bagenal, "*Jupiter: The Planet, Satellites and Magnetosphere", Cambridge University Press*, ISBN 0-521-81808-7

McGrath, M. A., Jia, X., Retherford, K., Feldman, P. D., Strobel, D. F., and Saur, J. (2013), "Aurora on Ganymede," *Journal of Geophysical Research*, Accepted Article, doi: 10.1002/jgra.50122

Neubauer, F. M. (1998), "The sub-Alfvénic interaction of the Galilean satellites with the Jovian magnetosphere", *Journal of Geophysical Research*, Vol. 103, pp. 19,843-19,866

Huba, J. D. (2009), "NRL Plasma Formulary", *Beam Physics Branch, Plasma Physics Division, Naval Research Laboratory, Washington D. C.*

Paranicas, C., et al. (1999), "Energetic particle observation near Ganymede", *Journal of Geophysical Research*, Vol. 104, No. A8, pp. 17,459-17,469

Ohtani, S-I., Fujii, R., Hesse, M., and Lysak, R. L. (2000), "Magnetospheric Current Systems", *American Geophysical Union, Monograph 118, Library of Congress Cataloguing-in-Publication Data*, Washington, Papers derived from presentations given at the AGU Chapman Conference on Magnetospheric Current Systems, Kona, Hawaii, 1999, ISBN 0-87590-976-0

Osterbrock, D. E., and Ferland, G. J. (1989), "Astrophysics of Gaseous Nebulae and Active Galactic Nuclei," *Second Edition, University Science Book*, ISBN 1-891389-34-3

Paty, C., and Winglee, R. (2004), "Multifluid simulations of Ganymede's magnetosphere", *Geophysical Research Letters*, Vol. 31, L24806, *doi:10.1029/2004GL021220*

Paty, C. (2006), "Ganymede's magnetosphere: Unraveling the Ganymede-Jupiter interaction through combining multifluid simulations and observations", *PhD Thesis, Department of Earth and Space Sciences, University of Washington, Seattle, WA, USA*

Paty, C., and R. Winglee (2006), "The role of ion cyclotron motion at Ganymede: Magnetic morphology and magnetospheric dynamics", *Journal of Geophysical Research*, Vol. 33, No. L10106, doi:10.1029/2005GL025273

Paty, C., W. Paterson, and R. Winglee (2008), "Ion energization in Ganymede's magnetosphere: Using multifluid simulations to interpret ion energy spectrograms", *Journal of Geophysical Research*, Vol. 113, No. A06211, doi:10.1029/2007JA012848

Piddington, J. H., and Drake, J. F. (1968), "Electrodynamic effects of Jupiter's satellite Io," *Nature*, Vol. 217, pp. 935-937

Retherford, K. (2002), "Io's Aurora, HST/STIS Observations," *PhD Thesis, Johns Hopkins University, Baltimore, MD, USA*

Retherford, K. (2009), "Ganymede UV Observations by New Horizons-Alice and HST-ACS", *Poster in the session "Satellites with Thin Atmospheres", Magnetospheres of Outer Planets, University of Cologne, Germany*

Russell, C.T. (2001), "The dynamics of planetary magnetospheres", *Planetary and Space Science*, Vol. 49, No. 10-11, pp. 1005-1030, doi:10.1016/S0032-0633(01)00017-4

Saur, J., Neubauer, F. M., Connerney, J. E. P., Zarka, P., and Kivelson, M. G. (2004), "Plasma Interaction of Io with its Plasma Torus", *Cambridge University Press, Edited by Bagenal, Dowling, and McKinnon*, pp. 537-560, 2007, Cambridge University Press, Cambridge, U.K

Serio et al. (2008), "The variation of Io's auroral footprint brightness with the location of Io in the plasma torus", *Icarus*, Vol. 197, pp. 368-374

Showman, A. P., and Malhotra, R. (1999), "The Galilean Satellites", *Science*, Vol. 286, No. 5437, pp. 77-84, doi:10.1126/science.286.5437.77

Schneider, N.M., and Trauer, J. T. (1995), "The structure of the Io torus", *Astrophysical Journal*, Vol. 450, pp. 450-462

Smith, E. (1999), "The Sun, Solar Wind, and Magnetic Field", *Proceedings of the International School of Physics Enrico FERMI Varenna*, Italy

Spencer et al. (2007), "Io Volcanism Seen by New Horizons: A Major Eruption of the Tvashtar Volcano", *Science*, Vol. 318, pp. 240-243, doi: 10.1126/science.1147621

Stein (1971), "Reflection, Refraction, and Coupling of MHD Waves at a Density Step", *The Astrophysical Journal, Supplement Series*, Vol. 22, No. 192, pp. 419-444

Stone, S. M., and T. P. Armstrong (2001), "Three-dimensional magnetopause and tail current model of the magnetosphere of Ganymede", *Journal of Geophysical Research*, Vol. 106. No. 10, pp. 21,263-21,275

Thorne, K. (unpublished data, 2008), "Magnetohydrodynamics", *Physics class 136, available from the California Institute of Technology, Division of Physics, Mathematics and Astronomy, Pasadena, California,* (http://www.pma.caltech.edu/Courses/ph136/yr2008/0817.2.K.pdf)

Tillack, M. S., and N. B. Morley (1998), "Magnetohydrodynamics", *McGraw Hill Standard Handbook for Electrical Engineers*, 14th edition, Library of the University of San Diego, Advanced Energy Technology Group, Center for Energy Research

Wilcox, J. M., Hoeksema, J. T., and Scherrer, P. H. (1980), "The origin of the warped heliospheric current sheet", *Stanford University, Institute for Plasma Research, CA, Defense Technical Information Center*, 10 pages

Wright (1987), "The interaction of Io's Aflvén waves with the Jovian magnetosphere", *Journal of Geophysical Research*, Vol. 92, No. A9, pp. 9963-9970